JVI Journals.ASM.org

Kallikrein-8 Proteolytically Processes Human Papillomaviruses in the Extracellular Space To Facilitate Entry into Host Cells

Carla Cerqueira,[a]* Pilar Samperio Ventayol,[a] Christian Vogeley,[a] Mario Schelhaas[a,b]

Emmy-Noether Group Virus Endocytosis, Institutes of Molecular Virology and Medical Biochemistry, ZMBE, University of Münster, Münster, Germany[a]; Cluster of Excellence EXC1003 Cells in Motion, Münster, Germany[b]

ABSTRACT

The entry of human papillomaviruses into host cells is a complex process. It involves conformational changes at the cell surface, receptor switching, internalization by a novel endocytic mechanism, uncoating in endosomes, trafficking of a subviral complex to the Golgi complex, and nuclear entry during mitosis. Here, we addressed how the stabilizing contacts in the capsid of human papillomavirus 16 (HPV16) may be reversed to allow uncoating of the viral genome. Using biochemical and cell-biological analyses, we determined that the major capsid protein L1 underwent proteolytic cleavage during entry. In addition to a dispensable cathepsin-mediated proteolysis that occurred likely after removal of capsomers from the subviral complex in endosomes, at least two further proteolytic cleavages of L1 were observed, one of which was independent of the low-pH environment of endosomes. This cleavage occurred extracellularly. Further analysis showed that the responsible protease was the secreted trypsin-like serine protease kallikrein-8 (KLK8) involved in epidermal homeostasis and wound healing. Required for infection, the cleavage was facilitated by prior interaction of viral particles with heparan sulfate proteoglycans. KLK8-mediated cleavage was crucial for further conformational changes exposing an important epitope of the minor capsid protein L2. Occurring independently of cyclophilins and of furin that mediate L2 exposure, KLK8-mediated cleavage of L1 likely facilitated access to L2, located in the capsid lumen, and potentially uncoating. Since HPV6 and HPV18 also required KLK8 for entry, we propose that the KLK8-dependent entry step is conserved.

IMPORTANCE

Our analysis of the proteolytic processing of incoming HPV16, an etiological agent of cervical cancer, demonstrated that the capsid is cleaved extracellularly by a serine protease active during wound healing and that this cleavage was crucial for infection. The cleavage of L1 is one of at least four structural alterations that prime the virus extracellularly for receptor switching, internalization, and possibly uncoating. This step was also important for HPV6 and HPV18, which may suggest that it is conserved among the papillomaviruses. This study advances the understanding of how HPV16 initially infects cells, strengthens the notion that wounding facilitates infection of epidermal tissue, and may help the development of antiviral measures.

Human papillomaviruses (HPVs) comprise a large family of small, nonenveloped DNA viruses with transforming potential. HPVs selectively infect basal keratinocytes of stratified skin and mucosal epithelia and persist, mostly without clinical symptoms, in virtually every part of the human skin. The biological costs of HPV persistence range from benign papilloma and genital warts over preneoplastic lesions to anogenital or oropharyngeal cancers (1). In fact, infection by the so-called "high-risk" HPV causes about 5% of all human cancers (2). Of these, cervical cancers are the most prevalent. However, HPV-associated oropharyngeal squamous cell carcinomas and anal cancers have dramatically increased in both men and women over the last 30 years (3).

The biology of HPV is unique. The multistep process of HPV entry involves a protracted extracellular residence on the extracellular matrix or cells after virus binding, uptake by a novel endocytic mechanism, and nuclear import of viral genomes during mitosis (4, 5). Furthermore, replication and assembly of new virions are restricted to terminally differentiating keratinocytes (1). The HPV particle is composed primarily of the major capsid protein, L1. L1 is necessary and sufficient to build the icosahedral (T=7) virion, which is formed by 72 homopentamers of L1. If L1 is expressed together with the minor capsid protein, L2, the two proteins coassemble the particle around chromatinized viral DNA (vDNA) (6). Particle stability is achieved by extensive hydrophobic interactions between the five L1 molecules forming the capsomers. The capsomers are linked by the invading C-terminal arm of an L1 molecule from a neighboring capsomer (7, 8). In addition, papillomaviruses undergo, like many other viruses, a maturation process after initial assembly. During this maturation intermolecular disulfide bonds between L1 molecules are formed that covalently link adjacent pentameric capsomers (7, 9, 10).

The transmission between infected and uninfected cells of the HPV particle is not well understood. It involves the reversal of

Received 27 January 2015 **Accepted** 20 April 2015

Accepted manuscript posted online 29 April 2015

Citation Cerqueira C, Samperio Ventayol P, Vogeley C, Schelhaas M. 2015. Kallikrein-8 proteolytically processes human papillomaviruses in the extracellular space to facilitate entry into host cells. J Virol 89:7038–7052. doi:10.1128/JVI.00234-15.

Editor: M. J. Imperiale

Address correspondence to Mario Schelhaas, schelhaas@uni-muenster.de.

* Present address: Carla Cerqueira, Laboratory of Cellular Oncology, National Cancer Institute, National Institutes of Health, Bethesda, Maryland, USA.

C.C. and P.S.V. contributed equally to this article.

doi:10.1128/JVI.00234-15

capsid stability during entry into target cells to eventually release the viral genome at the site of replication, a process termed uncoating. Generally, uncoating occurs through interaction with the cellular environment, i.e., different chemical milieus or specific interactions with cellular proteins. Thereby, stabilizing contacts in the virus structure are modified through conformational changes, isomerization of covalent bonds, refolding, and/or proteolysis (11).

Due to the difficulties associated with growing HPV in differentiating tissue, most of what is known about the early steps in the virus life cycle has been learned by a surrogate infection system, the so-called pseudoviruses (PsV). PsV are virus-like particles containing a pseudogenome that is capable of expressing reporter genes, the expression of which indicates a successful infection (12). Most of the existing knowledge is based on HPV16, the most prevalent high-risk HPV, which has often served as a paradigm for the papillomaviruses.

After the virus assembles and accesses the target cells, entry of HPV16 into host cells starts with binding to heparan sulfate proteoglycans (HSPGs) that are situated within the plasma membrane or the extracellular matrix (ECM) (13–18). Alternatively, the virus can bind to laminin-332 as a transient binding receptor (15, 19–21). Interaction with HSPGs facilitates a first conformational change in the virus that appears to be critical for infection (19). Through interaction with cyclophilins, the amino-terminal part of the minor capsid protein L2 is externalized from the interior of the capsid structure (22) before the proprotein convertase furin cleaves off an N-terminal proximal peptide of L2 to expose the so-called RG-1 epitope (23, 24). These changes are thought to facilitate the transfer of a virus particle to an elusive secondary receptor or receptor complex (21, 24, 25). The viral particles are then internalized by a novel endocytic mechanism that routes the virus to the endosomal pathway (26). Here, the majority of the L1 capsomers are removed from a subviral complex that contains L2 and the viral nucleosomes by the action of cyclophilin B (27). Prior to membrane penetration and nuclear import, the subviral particles are trafficked to the trans-Golgi network (TGN) (28, 29). Nuclear import of the viral genome occurs during mitosis through association with metaphase chromosomes (4).

Despite these findings, our understanding of the uncoating process remains fragmented. For example, the potential role of the structural change induced by interaction with heparan sulfates remains elusive. In addition, it remains unclear how the covalent interpentameric disulfide bonds are broken, which would be a prerequisite to removing the pentameric capsomers from the subviral particles by cyclophilins. In addition to reduction or isomerization of the disulfides, a further mechanism to unlink pentamers may be proteolytic processing of L1 in the endosomal pathway, which has been previously observed (30–33). However, the role of L1 proteolysis for HPV infection is still under debate since different studies reached divergent conclusions on the necessity of L1 proteolysis for infection. Hence, this study readdressed the role of proteolytic processing of the major capsid protein in HPV16 entry.

MATERIALS AND METHODS

Cell lines, antibodies, and reagents. HeLa cells were from the ATCC. HeLa Kyoto cells were a kind gift from L. Pelkmans (Institute of Molecular Life Sciences, Zurich, Switzerland) (34). HaCaT cells that originated from N. Fusenig (DKFZ, Heidelberg, Germany) (35) were a kind gift from the Schiller lab (NIH, National Cancer Institute, Bethesda, MD, USA). Protease inhibitor cocktail EDTA-free tablets (protease inhibitor mix) were from Roche. E-64, CA-074, CA-074Me, cathepsin L inhibitor I, and cyclosporine (CsA) were from Calbiochem. AEBSF [4-(2-aminoethyl)benzenesulfonyl fluoride], leupeptin, $ZnCl_2$, and $ZnSO_4$ were from Applichem. The inhibitors 3-methyladenine (3-MA), marimastat, batimastat, and heparin (H4784) were from Sigma. Dec-RVKR-CMK (decanoyl-Arg-Val-Lys-Arg-chloromethylketone) was from Bachem. Hoechst 33258, Alexa Fluor (AF)-conjugated carboxylic acid, and AF-conjugated secondary antibodies were from Life Technologies. The Bromo-2′-deoxy-uridine (BrdU) Labeling and Detection Kit I was from Roche. The L1-7 and RG-1 monoclonal antibodies were kind gifts from M. Sapp (Louisiana State University, Shreveport, LA, USA) (36) and from R. Roden (Johns Hopkins University, Baltimore, MD, USA) (37), respectively. The CAMVIR-1 and LAMP1 (H4A3) antibodies were from Santa Cruz Biotechnology, the monoclonal kallikrein-8 (KLK8) rabbit antibody (EPR5752) (2) was from Abcam, the TGN46 antibody (AHP1586) was from Abd Serotec, and the tubulin antibody (DM1A) was from Sigma. The rabbit serum was from Davids Biotechnologie GmbH.

Viruses. HPV6, HPV16, and HPV18 PsV containing a green fluorescent protein reporter plasmid (HPV6-GFP, HPV16-GFP, and HPV18-GFP, respectively) were produced as previously described using plasmids p6LLw, p16SheLL, and p18LLw, respectively, and pCIneo (12, 38–40). For HPV16 PsV containing BrdU-labeled DNA (BrdU-HPV16) or 5-ethynyl-2′-deoxyuridine (EdU)-labeled DNA (EdU-HPV16), cells were incubated with BrdU or EdU, respectively, during virus production according to a previously described protocol (41). Fluorophore-labeled HPV16 PsV were prepared as described previously (42). Briefly, HPV16 PsV were incubated at a 1:1 molar ratio (L1/dye) with AF-conjugated carboxylic acid for 1 h at room temperature. Viruses were separated from free dye by size exclusion chromatography. Vaccinia virus (VV) expressing GFP from an early/late promoter (VV-GFP) was kindly provided by J. Mercer (43).

RNAi. Predesigned small interfering RNA (siRNA) oligonucleotides directed against human KLK8 (KLK8_1, SI00095354; and KLK8_2, SI00095368) and the AllStars negative-control siRNA (AllStarNeg; SI03650318) were from Qiagen. For RNA interference (RNAi), 3.5×10^4 HeLa ATCC or HaCaT cells or 2×10^4 HeLa Kyoto cells were reverse transfected with 10 nM siRNAs (HeLa) or 20 nM (HaCaT) siRNA using Lipofectamine RNAiMax (Life Technologies) according to the manufacturer's instructions. Subsequently, at 48 h posttransfection cells were infected or cell lysates for Western blotting were prepared. Cell lysates were prepared by the addition of 2.5× SDS loading buffer. After a 10-min denaturation at 95°C, the samples were analyzed for the amount of KLK8 or, as a loading control, that of tubulin by SDS-PAGE and Western blotting. The relative amount of KLK8 was determined by the normalized signal intensities of the KLK8 band. For this, the signal intensities were determined using ImageJ (version 1.49k; National Institutes of Health), normalized to the loading control, and related to the intensities of the AllStarNeg control.

Infectivity studies. About 16 h prior to experimentation, 5×10^4 HeLa or HaCaT cells were seeded in 12-well plates. Cells were pretreated for 30 min with the concentrations of protease inhibitors or solvent in growth medium indicated in the figure legends. Subsequently, 1.5 to 3.5 ng of HPV16 PsV was added to medium containing inhibitors or solvent to result in about 20% of GFP-expressing cells for the unperturbed control and corresponding to about 50 to 150 particles per cell. The inoculum was exchanged at 2 h postinfection (p.i.) with fresh medium containing inhibitors or solvent. The medium was exchanged for 20 mM NH_4Cl (10 mM HEPES, pH 7.4) at 12 h p.i. Alternatively, RNAi-treated cells were infected with 1.5 to 2.5 ng of HPV16, 690 ng of HPV6, 85 ng of HPV18 PsV, or VV (1 PFU/cell). Cells were infected 48 h post-siRNA transfection, where the inoculum was exchanged at 2 h p.i. For infection assays in the presence of antibodies, antibodies directed against KLK8 or a control rabbit serum were added to 500 μl of medium 30 min before infection. Subsequently, 2

ng of HPV16 PsV was added to medium containing the antibodies. The inoculum was exchanged at 12 h p.i. for medium containing 10 mM NH_4Cl. At 48 h p.i., cells were trypsinized and fixed in 4% (wt/vol) paraformaldehyde (PFA) in phosphate-buffered saline (PBS). The number of infected cells (GFP-expressing cells) was determined by flow cytometry (FACSCalibur; Beckton Dickson) and normalized relative to the number in solvent-treated or AllStarNeg siRNA-transfected controls.

Proteolytic processing of L1 in cells. About 16 h prior to experimentation, 1×10^5 HeLa or HaCaT cells were seeded in 12-well plates. Cells were infected with 4 ng of HPV16-GFP in the presence or absence of protease inhibitors after pretreatment as described above. At the time points indicated in the figure legends, cells were washed with PBS and subsequently lysed by the addition of 2.5× SDS loading buffer. Samples were denatured for 10 min at 95°C. L1 processing was analyzed by SDS-PAGE and Western blotting using the CAMVIR-1 antibody.

Fluorescence time course of labeled HPV16 and L1-7 staining. About 16 h prior to infection, 5×10^4 HeLa or HaCaT cells were seeded on coverslips in 12-well plates. Cells were infected with about 50 to 100 AF-labeled HPV16 particles per cell and fixed with PFA at 2, 10, 16, and 24 h p.i. For further immunostaining of the L1-7 epitope, cells were fixed at 12 h p.i. and permeabilized with 0.1% Triton X-100. Phalloidin staining was performed in PHEM Triton buffer (60 mM PIPES [piperazine-*N*,*N*′-bis(2-ethanesulfonic acid)], 10 mM EGTA, 2 mM $MgCl_2$, 25 mM HEPES, pH 6.9, 0.1% Triton X-100) and Hoechst stain in PBS. Coverslips were mounted on Citifluor glycerol-PBS solution (Citifluor, Ltd., London, United Kingdom). Samples were imaged using the 63× objective of a spinning disc confocal microscope (Zeiss Axio Observer Z1, equipped with a Yokogawa CSU22 spinning disc module; Visitron Systems GmbH). Z-stacks covering the cell's volume were converted into maximum intensity z-projections using ImageJ (version 1.49k; National Institutes of Health). The number of virus signals per cell from at least five fields of view was determined by image segmentation from the maximum intensity projection. The cell area was determined using phalloidin staining for segmentation. Similarly, the mean fluorescence intensities were measured as arbitrary units after background subtraction.

Uncoating and trafficking of viral DNA and HPV16 particles. For the analysis of HPV16 uncoating, 3×10^4 HeLa Kyoto cells were seeded 16 h before infection with BrdU-HPV16 (500 to 1,000 viral genome equivalents/cell). The cells were fixed at 20 h p.i. in ice-cold 70% ethanol containing 15 mM glycine. Cells were stained using the Bromo-2′-deoxyuridine Labeling and Detection Kit I (Roche) according to the manufacturer's instructions with the exception that an Alexa Fluor label secondary antibody was used. For the analysis of vDNA trafficking, HeLa Kyoto cells were transfected with siRNA as described above. After 48 h cells were infected with EdU-HPV16 (500 to 1,000 viral genome equivalents/cell) and fixed with PFA at 20 h p.i. Cells were stained with a Click-iT EdU Alexa Fluor 488 imaging kit (Life Technologies) according to the manufacturer's instructions. Subsequently, cells were immunostained against TGN46 or LAMP1. Alternatively, RNAi-treated HeLa Kyoto cells were infected at 48 h posttransfection with 100 to 300 AF-labeled HPV16 particles/cell, fixed at 8 h p.i., and immunostained against LAMP1 for the analysis of subcellular localization of HPV16. The samples were imaged as z-stacks covering the volume of cells using a 63× objective of an LSM 780 confocal microscope (Zeiss). To quantify uncoating, the mean intensity of BrdU signal (uncoated vDNA) per cell was determined as described above. Colocalization of vDNA or AF-labeled HPV16 PsV and cell nuclei (Hoechst), the TGN (TGN46), or late endosomes (LAMP1) was determined using the Imaris colocalization module (version 7.6.4). At least 10 cells per sample were analyzed for each of three independent experiments.

RG-1 exposure. To analyze the exposure of the RG-1 epitope, 1.5×10^4 HeLa Kyoto cells were reverse transfected with siRNAs as described above in eight-well microscopy chambers (Ibidi). Cells were infected with 100 ng of HPV16 PsV at 48 h after transfection. The inoculum was exchanged for growth medium at 1 h p.i. The cells were immunostained for the RG-1 epitope at 4 h p.i. as described previously (24). Briefly, cells were subsequently incubated with RG-1 and an AF488-labeled secondary antibody for 1 h, after which cells were fixed with 2% PFA. Image acquisition and analysis occurred as described for the fluorescence time course of labeled HPV16 (see above). Here, 20 fields of view/sample/experiment were analyzed. Values are reported as the RG-1 signal relative to untreated or AllStarNeg siRNA-transfected cells.

***In vitro* proteolysis.** ECM-covered coverslips were freshly prepared as described previously (19). Briefly, cells were removed by incubation in PBS containing 10 mM EDTA and by gentle pipetting. The ECM remaining in the well was washed with PBS to remove cellular debris prior to binding of PsV. HPV16 PsV (20 ng/coverslip) were either preincubated with 10 mg/ml heparin or left untreated for 2 h at room temperature. The virus was bound to the ECM-covered coverslips for 2 h and incubated with medium containing secreted cellular material (conditioned medium) or Dulbecco's modified Eagle medium supplemented with 10% fetal calf serum ([FCS] DMEM-10) for 12 h. Conditioned medium was prepared by harvesting the supernatants of HaCaT cells grown for 72 h and stored at 4°C. Inhibitor (protease inhibitor mix, leupeptin, batimastat, marimastat, dec-RVKR-CMK, E-64, AEBSF, or CsA) or Zn^{2+} was added to the conditioned medium immediately prior to addition to the ECM-bound virus. The concentrations of inhibitor/Zn^{2+} that were used are described in the figure legends.

Depletion of KLK8 from conditioned medium was achieved by incubation with KLK8 antibody (7.7 μg/ml) for 2 h and subsequent precipitation using protein G-agarose beads.

At 12 h after the addition of conditioned medium, ECM-bound virus was washed with PBS and subsequently lysed by the addition of 2.5× SDS loading buffer. Samples were denatured for 10 min at 95°C. L1 processing was analyzed by SDS-PAGE and Western blotting using the CAMVIR-1 antibody.

Overseeding experiments. The overseeding experiments were carried out as previously described (19). ECM was prepared as described above, and 1.25 ng of HPV16 PsV was bound to the ECM. ECM-bound HPV16 PsV were treated with conditioned medium or DMEM-10 for 12 h. At 48 h post-siRNA transfection of HeLa cells, they were briefly trypsinized and counted. A total of 2×10^4 cells were seeded over the ECM-bound PsV. At 48 h after overseeding, the cells were trypsinized and fixed in 4% PFA. The number of infected cells was determined by flow cytometry. The percentage of infected cells per sample was normalized to number of AllStarNeg-transfected cells seeded over ECM-bound PsV treated with DMEM-10.

RESULTS

HPV16 L1 is proteolytically cleaved during infection. Previous reports indicate proteolytic processing of HPV16 L1 during cell entry (30–32). To analyze the potential contribution of cellular proteases to proteolytic processing and uncoating of HPV16, we first followed the cleavage pattern of L1 during entry into HeLa and HaCaT cells. At different time points post-HPV16 infection, cell lysates were analyzed by SDS-PAGE and Western blotting. L1 bands were detected with the CAMVIR-1 antibody directed against amino acids (aa) 204 to 210 (44). In HeLa cells a band of about 45 kDa was observed in samples from uninfected cells, which suggested the unspecific detection of a cellular protein by the CAMVIR-1 antibody (Fig. 1A, asterisk). HaCaT cells exhibited two additional unspecific bands at around 52 and 50 kDa (Fig. 1B, asterisks). Over the time course of infection, a progressive decrease of full-length L1 was observed from 100% at 2 h p.i. to 65% at 12 h p.i. to 40% at 48 h p.i. (Fig. 1C) that indicated proteolytic processing of L1, consistent with previous reports (Fig. 1A) (30, 31). Several cleavage bands were observed ranging from about 50 to 15 kDa (Fig. 1A). We designated the putative cleavage products according to their decreasing molecular masses as L1 A to I. Of these, only L1 H and I have been previously described (30, 31).

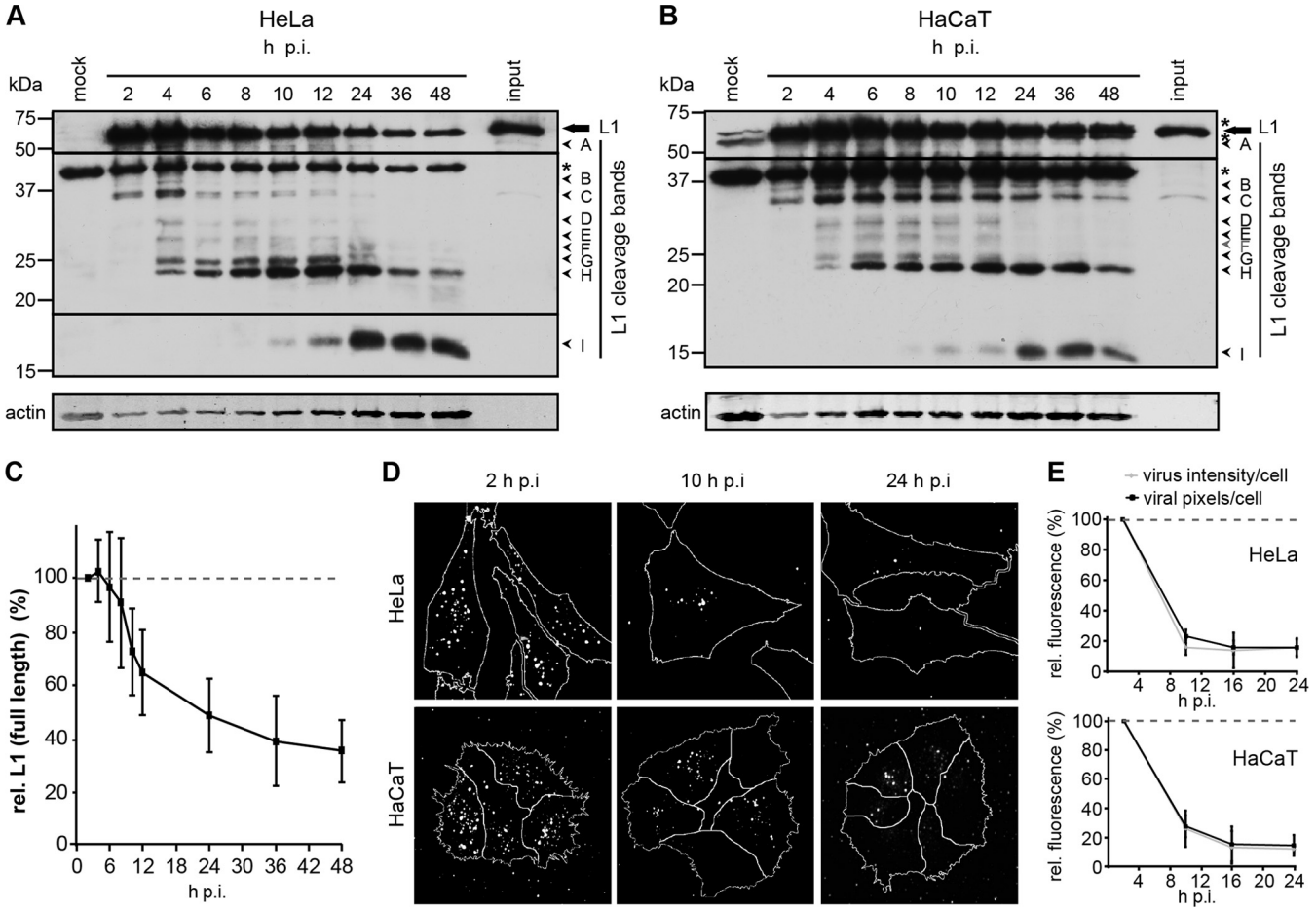

FIG 1 HPV16 L1 is proteolytically processed during cell entry. HeLa (A) or HaCaT (B) cells were infected with HPV16 PsV. Cells were lysed at different times p.i. The samples were subjected to SDS-PAGE and analyzed by Western blotting using the CAMVIR-1 antibody directed against L1. Indicated are the L1 full-length signal (L1) and the lower-molecular-mass signals that were termed A to I. The unspecific detection of signal in uninfected cells is marked by an asterisk. The lowest blot shows the loading control (actin). (B) L1-F is absent but marked in gray to highlight the cleavage product observed in HeLa cells. (C) Quantification of the L1 full-length signal from panel A. Data are the means of three independent experiments ± standard deviations. Error bars for the 36- and 48-h time points p.i. indicate the variation between two experiments. Values are shown in percent relative (rel) to value for the 2-h time point p.i. (D) HeLa or HaCaT cells were infected with fluorescently labeled HPV16 PsV. At different times p.i., cells were fixed and subjected to microscopy analysis. Depicted are maximum projections of confocal sections at the indicated times. The cell outline was detected by phalloidin staining and is indicated by a white line. (E) Quantification of the HPV16 signal intensities and covered areas from panel D. Date are the means of three independent experiments ± standard deviations. Values are shown in percent relative to the value for the 2-h time point p.i.

Overall, there was little difference between HeLa and HaCaT cells (compare Fig. 1A and B); only the minor cleavage product L1 F was not detectable in HaCaT cells (Fig. 1B). Since the bands were detected progressively with time from higher to lower molecular masses, it appeared that distinct cleavages occurred with progression of entry.

When cells were infected with labeled HPV16 (AF488- or AF594-HPV16), a progressive decrease of fluorescence signal was observed over the time course of infection, consistent with proteolytic processing of L1 (Fig. 1D). The relative fluorescence signal decreased from 100% at 2 h p.i. to about 20% at 24 h p.i. (Fig. 1E). Since the fluorophore is covalently attached almost exclusively to the L1 protein (42), the decrease indicated degradation or proteolytic processing of L1.

Cysteine cathepsins cleave L1, but cleavage is dispensable for infection. Next, we aimed to determine which proteases were responsible for the cleavages. To analyze the relative contribution of certain proteases, cells were infected in the presence or absence of small compound inhibitors. Cells were lysed at 12 h p.i., when most cleavage products were detectable, and analyzed as described above by Western blotting. To control for the detection of L1-unrelated bands by the CAMVIR-1 antibody, samples of uninfected cells in the presence of inhibitors were analyzed, but no further unspecific signals were observed in addition to the signals described above (data not shown).

Since HPV16 requires a low-pH-dependent step during entry that is most likely related to the passage through the endosomal pathway (26, 45–48) and since many endosomal proteases exhibit a low-pH optimum for enzymatic activity (49, 50), we initially analyzed the contribution of low pH to cleavage of L1. When the intraendosomal pH of HeLa cells was neutralized by NH_4Cl or bafilomycin A1 (Baf A1), the generation of most L1 cleavage products was inhibited (Fig. 2A). However, the L1 cleavage product L1 A of about 50 kDa accumulated. This suggested that most L1

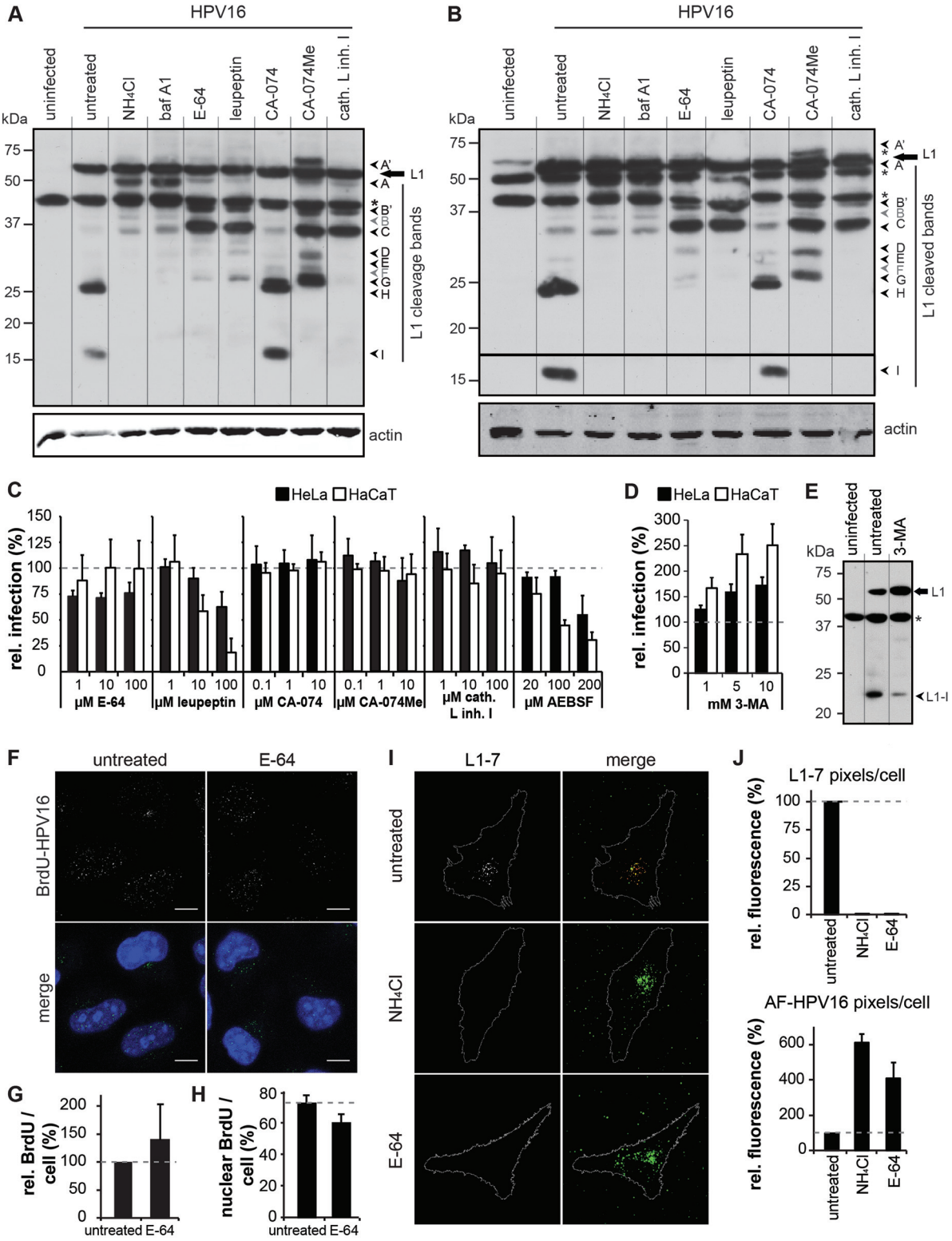

FIG 2 Inhibitory analysis of L1 proteolysis. HeLa (A) or HaCaT (B) cells were infected with HPV16 PsV in the presence or absence of the following inhibitors: NH_4Cl (20 mM), bafilomycin A1 (10 nM), E-64 (100 μM), leupeptin (100 μM), CA-074 or CA-074Me (20 μM), or cathepsin L inhibitor I (100 μM; cath L inh I). Cells were lysed at 12 h p.i. The samples were analyzed by SDS-PAGE and analyzed by Western blotting using the CAMVIR-1 antibody directed against L1. Indicated are the L1 full-length signal (L1) and the lower-molecular-mass signals A to I (compare Fig. 1A and B). In addition, newly appearing signals were termed A′ and B′. Signals B and F shown in Fig. 1A are not apparent and are therefore marked in gray. The lower blot shows the loading control (actin). Asterisks indicate unspecific signals. (C) HeLa or HaCaT cells were infected with HPV16-GFP in the presence or absence of inhibitors at the indicated concentrations. The number of GFP-expressing (infected) cells was determined at 48 h p.i. by flow cytometry. Depicted is the fraction of infected cells relative to the number of solvent-treated cells. Shown are the mean values for three independent experiments ± standard deviations. (D) HeLa or HaCaT cells were infected with HPV16-GFP in presence

cleavages required passage through the low-pH environment of endosomes and that, in addition, a pH-independent processing of L1 occurred.

Likely candidates for proteolytic processing and degradation within the endosomal pathway are cysteine cathepsins, lysosomal proteases that require acidic pH for activation (50, 51). The role of cysteine cathepsins in HPV entry has been previously analyzed with different results (23, 32, 33). Although two studies suggested a cathepsin-mediated cleavage of L1, Dabydeen and Meneses (33) claimed a productive role for it in virus uncoating, whereas Calton and colleagues (32) suggested a role for postuncoating degradation. To revisit the role of cathepsins in the generation of distinct L1 cleavage products and infection, we used several well-established cathepsin inhibitors. The general cysteine protease inhibitor E-64 (52) inhibited the generation of most cleavage products, whereas L1 C (35 kDa) accumulated (Fig. 2A). In addition, a new cleavage band was observed of about 43 kDa in size (L1 B′), and the pH-independent L1 A was also detectable. Leupeptin, a cysteine and serine protease inhibitor (53, 54), had the same effect as E-64 (Fig. 2A). The cell-permeable cathepsin L inhibitor I (Z-Phe-Phe-FMK [benzyloxycarbonyl-Phe-Phe-fluoromethylketone]) (55, 56) phenocopied the results observed with the more general inhibitors leupeptin and E-64, which may suggest that L1 is mostly processed by cathepsin L. In support of this notion, the generation of L1 cleavage products was only affected to a minor extent in the presence of the cell-permeable cathepsin B inhibitor CA-074Me that suppressed L1 I (57, 58) (Fig. 2A). Similar results were observed for HaCaT cells (Fig. 2B). Taken together, the results indicated that cysteine cathepsins were involved in proteolytic processing of HPV16 L1. In addition, three cleavage products accumulated in the presence of inhibitors. These are the low-pH-independent cleavage product L1 A, accumulating in the presence of endosomal acidification inhibitors, and the low-pH-dependent cleavage B′ and C products, accumulating in the presence of cathepsin inhibitors.

To analyze the role of cathepsins in infection, cells were pretreated with protease inhibitors for 30 min, infected with HPV16 PsV, and analyzed for reporter gene expression by flow cytometry at 48 h p.i. In HeLa cells, E-64 did not affect infection even at 100 μM, a comparatively high concentration (Fig. 2C). Neither of the cathepsin B inhibitors, CA-074 or the cell-permeable CA-074Me, affected infection (Fig. 2C). The cathepsin L inhibitor I also did not affect HPV16 infection (Fig. 2C). Similarly, infection of HaCaT cells was also unaffected by cathepsin inhibitors (Fig. 2C). In conclusion, cathepsin-mediated cleavage of L1 was not required for infection, supporting previous results (23, 32).

Since cathepsin-mediated L1 cleavage was not required for infection, we wondered whether it would be mostly the result of antiviral responses such as autophagy, a process that leads to the degradation of dysfunctional cellular organelles or foreign (pathogenic) material through the action of lysosomes (59). Recent reports indicated that autophagy restricts HPV16 infection (30, 60). To address the role of autophagy in cleavage and infection, we used the inhibitor 3-methyladenine (3-MA). As expected, 3-MA led to a dose-dependent increase of HPV16 infection (Fig. 2D) (30, 60). In addition, 3-MA reduced the abundance of L1 cleavage products but did not entirely inhibit cleavage (Fig. 2E). Our results indicated that autophagy contributed to degradation of infectious HPV16. The cathepsin-mediated cleavage of L1 in the absence of autophagy is likely the result of postuncoating degradation of the major capsid protein, as previously suggested (32).

Uncoating occurs when cathepsin activity is inhibited. If cathepsin-mediated L1 degradation occurs after uncoating in endosomes, cathepsin inhibitors should not affect uncoating. To test this, we used HPV16 PsV for infection that had incorporated bromodeoxyuridine (BrdU) into the pseudogenome (BrdU-HPV16). After infection with BrdU-HPV16, the labeled DNA is only accessible to antibody staining once uncoating has occurred (41). When HeLa cells were infected with BrdU-HPV16, similar amounts of BrdU signal were detected at 20 h p.i. in E-64-treated and untreated cells, which indicated that uncoating occurred to similar extents (Fig. 2F and G). Moreover, there was no significant difference in the delivery of BrdU-HPV16 to the nuclei (Fig. 2F and H).

HPV16 uncoating has also been previously analyzed by the exposure of the L1-7 epitope (aa 329 to 339 of HPV16 L1) (36). The exclusively intracellular accessibility of this epitope suggests that it is exposed after virus uncoating (27, 31, 48, 61). When we analyzed L1-7 epitope exposure at 12 h p.i. in untreated cells, the epitope was readily detectable. As previously described (27), L1-7 epitope staining was not observed in the presence of NH_4Cl (Fig. 2I and J). Interestingly, E-64 treatment of cells suppressed L1-7 epitope staining and enhanced the signal from fluorescently labeled HPV16 (Fig. 2I and J). Since infection and DNA uncoating occurred in the presence of E-64, this suggested that L1-7 exposure marked cathepsin-mediated degradation rather than uncoating.

In conclusion, our results supported a role of cathepsin-mediated degradation of L1 after uncoating, in line with the interpretation by Calton and colleagues (32). In addition, we observed three additional L1 cleavages (L1 A, B′, and C) in the presence of cathepsin inhibitors that may support uncoating of the viral genome.

HPV16 is cleaved extracellularly by a serine protease. In contrast to the cathepsin-specific protease inhibitors, leupeptin inhib-

or absence of 3-MA at the indicated concentrations. Infection was analyzed and depicted as described for panel C. Shown are the values for three independent experiments ± standard deviations. (E) HeLa cells were infected with HPV16 PsV in presence or absence of 10 mM 3-methyladenine (3-MA; autophagy inhibitor). Samples were analyzed as described for panel A. An asterisk indicates unspecific signals. (F) HeLa cells were infected with BrdU-HPV16 in the presence of E-64 (100 μM) or solvent control (untreated). The cells were fixed at 20 h p.i. and immunostained for BrdU (green) to detect uncoated vDNA. The nucleus was visualized by Hoechst staining (blue). Depicted are maximum projections of confocal sections. Scale bar, 10 μm. (G) Quantification of the BrdU signal per cell relative to the untreated sample ± standard deviations. (H) Quantification of nuclear BrdU signal per cell relative to the untreated sample ± standard deviations. (I) HeLa cells were pretreated with solvent (untreated), NH_4Cl (20 mM), or E-64 (100 μM) and infected with AF488-labeled HPV16. Cells were fixed at 12 h p.i. and immunostained with an antibody detecting the L1-7 epitope (aa 329 to 339 of HPV-16 L1). Depicted are maximum projections of confocal sections with the L1-7 signal and the merge of AF488-HPV16 and L1-7 signals in the first and second columns, respectively. The cellular borders were detected by phalloidin staining and are indicated by a white line. (J) Quantification of HPV16 L1-7 epitope staining from panel I. The amounts of L1-7 and AF-HPV16 signals were determined in relation to the cell area as described in Materials and Methods. The results are depicted relative to those for the solvent-treated (untreated) cells. Represented are the mean values of three independent experiments ± standard deviations.

ited infection (Fig. 2C). Leupeptin inhibits serine proteases in addition to cathepsins (53, 54), which indicated the relevance of a serine protease for infection. To verify this, we used 4-(2-aminoethyl)benzenesulfonyl fluoride (AEBSF), an irreversible serine protease inhibitor (62). When HeLa or HaCaT cells were infected in the presence of AEBSF, infection was reproducibly reduced to a modest but significant extent (Fig. 2C). Of the proteolytic processing of L1 that occurred cathepsin independently, one cleavage occurred independently of a low endosomal pH (Fig. 2A, L1 A). As this cleavage was also observed in a very early stage of infection (2 to 4 h p.i.) (Fig. 1A), we surmised that it might occur extracellularly.

In order to test this, we used medium that contained secreted material from HaCaT cells that we termed conditioned medium (for details, refer to Materials and Methods). HPV16 PsV were bound to extracellular matrix (ECM) from HaCaT cells. This ECM-bound virus was then incubated with conditioned medium. Subsequently, the virus was analyzed by SDS-PAGE and by Western blotting (Fig. 3A). A minor band of about 50 kDa was observed that corresponded to the pH-independent cleavage (Fig. 2A and 3B, L1 A). Since the appearance of this band in conditioned medium could be blocked by addition of a protease inhibitor mix and leupeptin (Fig. 3B, third and fourth columns, respectively) and since incubation with cell culture medium, including fetal calf serum (DMEM-10), did not produce this band (Fig. 3B), we concluded that L1 was processed by a secreted protease from HaCaT cells.

However, the processing of L1 appeared to be inefficient under the experimental conditions as only minor amounts of the cleaved product were observed. One reason for this could be that a prerequisite for cleavage exists, such as a structural alteration of the HPV capsid. HPV16 binds primarily to HSPGs (summarized in reference 5). Recently, our group has reported the induction of a structural change in the HPV16 capsid upon interaction with highly sulfated HS glycosaminoglycans such as heparin (19). To test whether this structural change would render the virus more prone to proteolytic processing in conditioned medium, HPV16 particles were incubated with heparin prior to ECM binding and incubation with conditioned medium. Processing of L1 was highly pronounced after heparin preincubation (Fig. 3B), which suggested that the structural change in the HPV16 capsid induced by HS facilitated proteolytic processing. In the presence of heparin about 50% of the L1 was cleaved (Fig. 3B and C). Similar to virus that was not incubated with heparin, processing of L1 was suppressed by addition of a protease inhibitor mix or leupeptin (Fig. 3B and C). Processing of heparin-preincubated virus also did not occur upon incubation in fresh medium (Fig. 3B and C). Taken together, these results indicated that L1 was proteolytically processed by a secreted protease and that the processing was facilitated by prior interaction with HS glycosaminoglycans.

Several candidates for the extracellular, proteolytic processing of HPV16 exist, such as matrix metalloproteases, which are required for infection (63), and the proprotein convertase furin, which is known to process the minor capsid protein L2 during cell entry (23).

To test, whether these proteases would be involved in the extracellular cleavage of L1, viruses were treated as before in the presence of inhibitors of matrix metalloproteases and furin, i.e., batimastat/marimastat and dec-RVKR-CMK, respectively. As a negative control, we used E-64, the cysteine cathepsin inhibitor. Batimastat/marimastat, the dec-RVKR-CMK, and E-64 did not inhibit cleavage of L1 in conditioned medium (Fig. 3D and E), despite the fact that batimastat, marimastat, and the dec-RVKR-CMK reduced infection, as expected (Fig. 3F to H) (23, 63).

To test whether serine proteases may be involved in extracellular proteolytic processing, cleavage in conditioned medium was analyzed in the presence of AEBSF. Since AEBSF completely inhibited the cleavage (Fig. 3D and E), we concluded that a serine protease is responsible for proteolytic processing in extracellular medium. In summary, these results indicate that a secreted serine protease cleaves HPV16 L1 extracellularly and that this cleavage is facilitated by prior interaction with HS glycosaminoglycans.

Kallikrein-8 facilitates HPV16 infection and proteolytic processing. The next question we addressed was which secreted serine protease might have facilitated extracellular L1 cleavage. Assuming that extracellular processing of the HPV16 capsid would be important, we turned to the findings of two independent, large-scale RNA interference (RNAi) screens (4, 28). These recent screens analyzed which particular genes affect HPV16 infection. Of the several secreted proteases, only one secreted serine protease, namely, kallikrein-8 (KLK8), was identified by both screens as required for infection (4, 28). KLK8 belongs to the kallikrein superfamily of active serine proteases and is involved in a proteolytic cascade in human skin and mucosal epidermis (64, 65). In particular, it cleaves a number of ECM constituents, such as fibronectin and collagen, but also processes fibrinogen and kininogens, presumably during wounding and inflammation (64, 66, 67). Thus, KLK8 appeared to be an interesting candidate for L1 cleavage.

We initially confirmed the importance of KLK8 for HPV16 infection. For this, HeLa cells were subjected to RNAi for 48 h, followed by infection with HPV16 and, as control, with VV, a large, enveloped poxvirus that enters cells by macropinocytosis (43). HPV16 infection of HeLa cells was reduced by 62% ± 16% and 73% ± 7% for the two independent siRNAs (Fig. 4A), which correlated with the extent of KLK8 knockdown on the protein level (Fig. 4C). Similar results were obtained in HaCaT cells (Fig. 4B and C). In contrast, VV infection of HeLa cells was unperturbed (Fig. 4A), suggesting an HPV-specific requirement of KLK8 for infection. To confirm that KLK8 is a crucial factor for HPV16 infection, HaCaT cells were infected in the presence of a rabbit antibody (EPR5752) (2) directed against KLK8. HPV16 infection was decreased in a dose-dependent manner by up to 52% ± 6%, whereas the control serum did not affect infection (Fig. 4D), which indicated that the secreted pool of KLK8 was important for infection. Since kallikreins are inhibited by the presence of Zn^{2+} ions (68), we also tested whether Zn^{2+} salts would affect infection. Millimolar concentrations of $ZnCl_2$ or $ZnSO_4$ reduced infection by up to 90% (Fig. 4E). All of these results pointed to an important role of KLK8 in HPV16 infection.

Next, the potential involvement of KLK8 in proteolytic processing of HPV16 PsV was tested. For this, PsV were bound to ECM as described above and treated with conditioned medium in the presence or absence of millimolar concentrations of Zn^{2+}. The presence of $ZnCl_2$ completely inhibited the extracellular cleavage of L1 (Fig. 4F and G). To further substantiate that cleavage would be mediated by KLK8, the conditioned medium was immunodepleted for KLK8. The conditioned medium was incubated with an antibody directed against KLK8 or a control antibody, and the complexes were removed from the solution using protein G-aga-

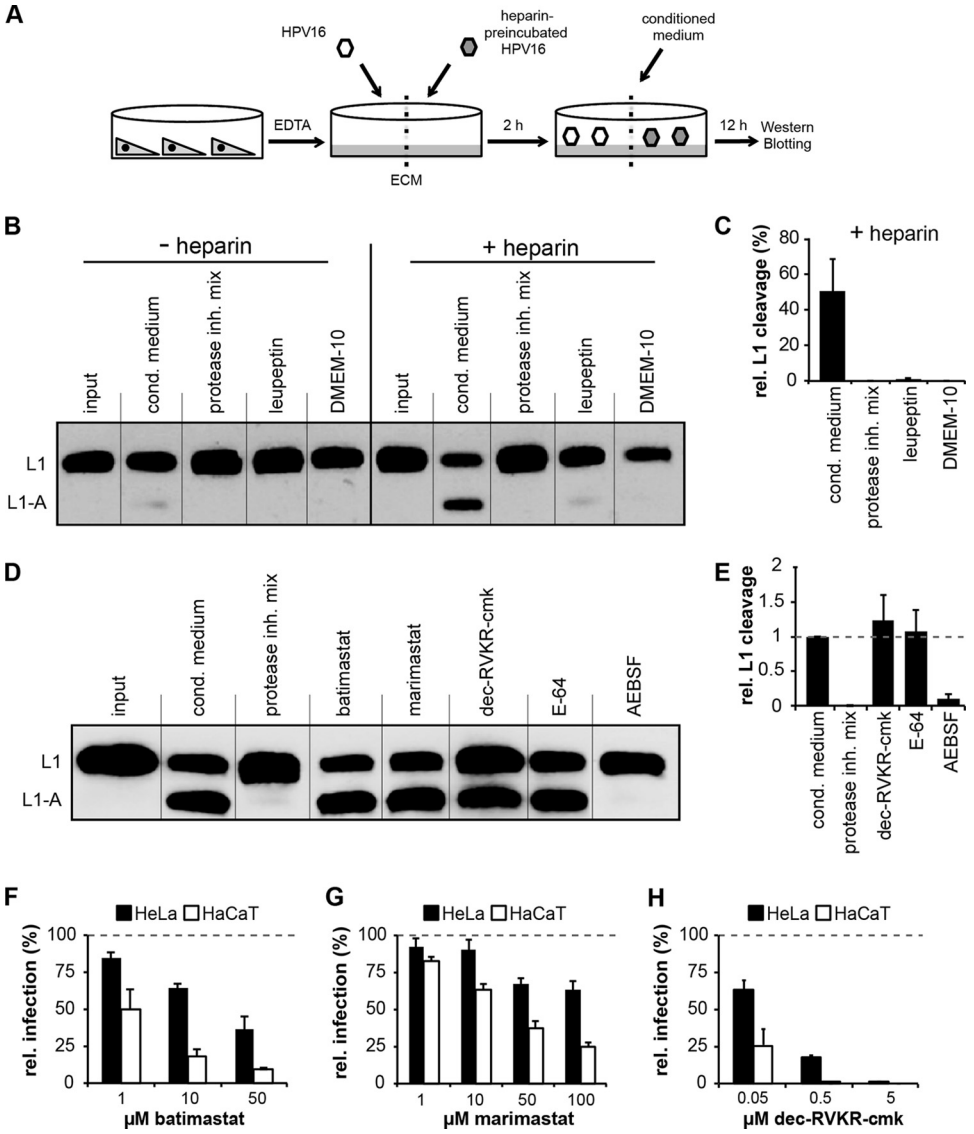

FIG 3 HPV16 L1 is proteolytically processed in conditioned medium by a serine protease. (A) Schematic depiction of the experimental strategy. HPV16 PsV were preincubated with 10 mg/ml heparin or solvent. Subsequently, the virus was allowed to bind to ECM obtained from HaCaT cells for 2 h at 37°C. The bound virus was incubated for 12 h at 37°C with conditioned medium in the presence or absence of inhibitors. Samples were lysed and subjected to SDS-PAGE and Western blotting using the CAMVIR-1 antibody directed against L1. (B) Depiction of Western blot from samples prepared as described for panel A with conditioned (cond) medium containing protease inhibitor (inh) mix (according to the manufacturer's instructions) and leupeptin (100 μM) or as a control with fresh medium (DMEM-10). The input sample was harvested after virus binding to ECM prior to incubation with medium. (C) Quantification of the generation of L1 A with heparin-preincubated HPV16 from the experiment shown described in panel B. Values are the signal intensities of L1 A relative to the total L1 signal (full-length L1 and L1 A). Data are the means of three independent experiments ± standard deviations. (D) The experiment is similar to that described for panel B, with the following inhibitors: batimastat (50 μM; matrix metalloproteases), marimastat (100 μM; matrix metalloproteases), dec-RVKR-CMK (5 μM; furin inhibitor), E-64 (100 μM; cathepsins), and AEBSF (200 μM; serine proteases). (E) Quantification of the samples from the experiment shown in panel D. Values are the relative amounts of L1 A signal intensities normalized to the value for the sample with conditioned medium without inhibitors. Data are the means of three independent experiments ± standard deviations. (F to H) HeLa or HaCaT cells were infected with HPV16-GFP in the presence of the matrix metalloprotease inhibitors batimastat and marimastat or the furin inhibitor dec-RVKR-CMK at the indicated concentrations. The number of GFP-expressing (infected) cells was determined at 48 h p.i. by flow cytometry. Depicted is the fraction of infected cells relative to the number of solvent-treated cells. Values are the means for three independent experiments ± standard deviations.

rose beads (Fig. 4H). The ECM-bound virus was then incubated with the resulting immunodepleted medium and analyzed as above. Incubation with medium depleted of KLK8 reduced the abundance of the cleavage product by 70% ± 16% (Fig. 4I), which indicated that KLK8 was responsible for the L1 processing.

KLK8 in the conditioned medium proved to be below the detection limits of Western blotting. Therefore, the presence of KLK8 was indirectly verified using cells depleted of KLK8 by RNAi. These cells were seeded on top of ECM-bound virus incubated with conditioned medium or, as control, with fresh medium. As described in the legend of Fig. 4J, RNAi against KLK8 reduced infection of virus incubated with fresh medium. In contrast, the presence of conditioned medium restored HPV16 infection in KLK8 knockdown cells, which suggested that the KLK8

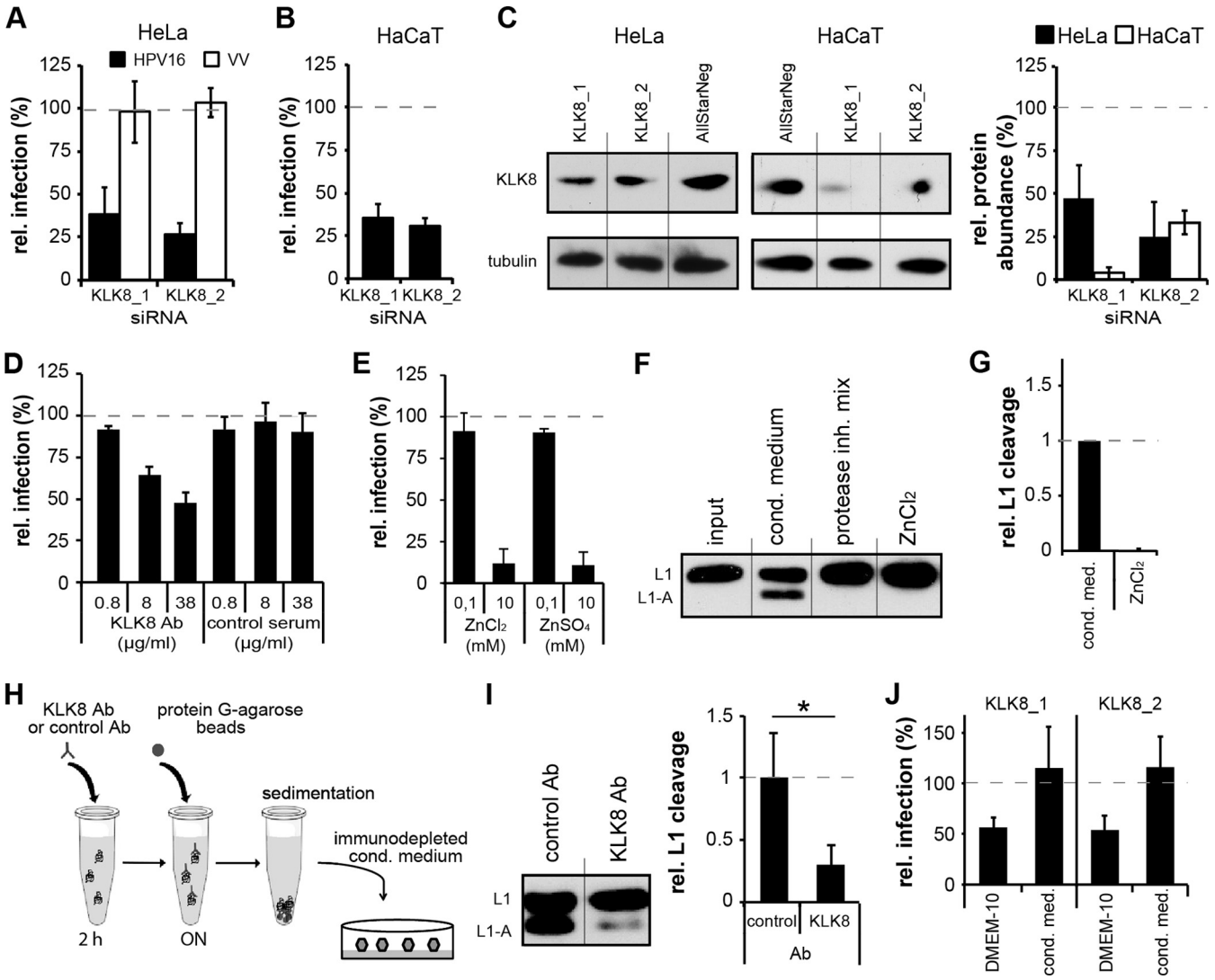

FIG 4 Kallikrein-8 is required for HPV16 infection and mediates L1 processing. (A) HeLa cells were reverse transfected with 10 nM siRNAs directed against KLK8 or the nontargeting control siRNA (AllStarNeg). Cells were infected with HPV16-GFP or VV at 48 h posttransfection. The number of GFP-expressing (infected) cells was determined at 48 h p.i. by flow cytometry. Depicted is the fraction of infected cells relative to the number of negative-control cells. Values are the means for three independent experiments ± standard deviations. (B) The experiment is as described for panel A using HaCaT cells and 20 nM siRNAs. Cells were infected with HPV16-GFP and analyzed as described for panel A. (C) HeLa or HaCaT cells were reverse transfected as described for panels A and B. Cells were lysed at 48 h posttransfection. KLK8 was detected in the samples after SDS-PAGE and Western blotting with an antibody directed against KLK8 (upper row). The Western blot against tubulin was used as a loading control (lower row). The quantification shows the signal of KLK8 relative to that of the negative control. Values are the means of three independent experiment ± standard deviations (right). (D) HaCaT cells were infected with HPV16-GFP in the presence of the indicated concentrations of KLK8 antibody (Ab) or control serum. The inoculum was exchanged for medium containing 10 mM NH_4Cl at 12 h p.i. The number of GFP-expressing (infected) cells was determined at 48 h p.i. by flow cytometry. Depicted is the fraction of infected cells normalized relative to the number of solvent-treated cells. Values are the means for three independent experiments ± standard deviations. (E) HeLa cells were infected with HPV16-GFP in the presence or absence of the indicated concentrations of $ZnCl_2$ or $ZnSO_4$. The inoculum was exchanged at 12 h p.i. for medium containing NH_4Cl (10 mM). The number of GFP-expressing (infected) cells was determined at 48 h p.i. by flow cytometry. Shown is the fraction of infected cells normalized relative to the number of solvent-treated cells. Values are the means for three independent experiments ± standard deviations. (F) Proteolytic processing of HPV16 L1 in conditioned medium as described in the legend of Fig. 3 with heparin-preincubated HPV16 in the presence of protease inhibitor mix or the indicated concentrations of $ZnCl_2$. (G) Quantification of the generation of L1 A with heparin-preincubated HPV16 from the experiment shown in panel F. Given are the relative amounts of L1 A signal intensities normalized to the value for the sample with conditioned medium without inhibitors. Data are the means of three independent experiments ± standard deviations. (H) Schematic depiction of immunodepletion of KLK8 from conditioned medium. Incubation of conditioned medium with KLK8 or control antibody was followed by addition of protein G-agarose beads. After sedimentation of the complexes, the resulting supernatant was used as immunodepleted conditioned medium. (I) The experiment is as described in the legend of Fig. 3, using KLK8 immunodepleted or control depleted medium. The quantified signal intensities of L1 A are given relative to those of the samples that were depleted as a control. Values are the means of three independent experiments ± standard deviations. Statistical significance was determined by a two-tailed, independent *t* test (*, $P \leq 0.05$). (J) HeLa cells were subjected to RNAi as described for panel A. Heparin-preincubated HPV16-GFP bound to ECM from HaCaT cells was incubated with conditioned medium or DMEM-10 for 12 h. The siRNA-transfected cells were seeded on top of the ECM-bound HPV16-GFP. Subsequently, the number of GFP-expressing (infected) cells was determined at 48 h postseeding by flow cytometry. Depicted is the fraction of infected cells relative to the number of negative-control cells. Values (percentages) are the means of three independent experiments ± standard deviations.

present in conditioned medium compensated for the reduced expression in siRNA-treated cells.

In summary, these results established that the secreted serine protease KLK8 proteolytically processed the L1 protein in HPV16 PsV and that this cleavage facilitated infection.

KLK8 is involved in the exposure of the RG-1 epitope and internalization of the virus. Finally, the role of the extracellular processing of L1 for HPV16 entry was addressed. We first tested a late step during the entry process, the intracellular transport of the viral DNA (vDNA) to the Golgi complex prior to nuclear import (28, 29). HeLa cells were depleted of KLK8 and then infected with HPV16 PsV that contained vDNA labeled with the nucleotide analogue EdU (EdU-HPV16). At 20 h p.i., cells were fixed and stained for the vDNA using Click-iT chemistry and with an antibody directed against TGN46, a marker for the Golgi complex (69). As expected, the vDNA accumulated perinuclearly with an apparent colocalization with the Golgi marker or the nucleus in cells treated with the control siRNA (Fig. 5A, C, and D) (29). As a control, cells were treated with Baf A1, which blocks uncoating of HPV16 in endosomes and prevents further transport of the subviral complex containing the vDNA (27). In bafilomycin-treated cells, the vDNA was found perinuclearly without any apparent overlap with the Golgi marker or the nucleus, as expected (Fig. 5A, C, and D). In contrast, the vDNA was dispersedly localized in cells treated with siRNAs directed against KLK8, with significantly reduced levels of overlap with the Golgi marker or nucleus (Fig. 5A, C, and D). Moreover, the localization of fluorescently labeled HPV16 particles in KLK8 knockdown cells exhibited a decreased overlap with LAMP1-positive endosomes (Fig. 5B and E). These results indicated a defect of virus trafficking to endosomes and the Golgi complex in cells depleted of KLK8. The dispersed localization of the viral particles and the vDNA was also consistent with a defect in internalization or a very early intracellular trafficking defect of the virus in KLK8-depleted cells.

This defect in internalization could mean that proteolytic processing of L1 by KLK8 has an impact on the structural changes in HPV16 virions that lead to engagement of a putative secondary receptor. These changes involve the externalization of L2 by the chaperon cyclophilin B and proteolytic cleavage of L2 by furin, which eventually result in the exposure of the RG-1 epitope of L2 (22, 24). To verify this hypothesis, the extent of RG-1 epitope exposure was tested in cells depleted of KLK8. The RG-1 epitope was readily detectable in cells treated with control siRNA (Fig. 5F and G), whereas in cells that were treated with cyclosporine (CsA), an inhibitor of cyclophilins, no staining was detectable, as expected (Fig. 5F and G) (22). In cells depleted of KLK8, the RG-1 epitope exposure was reduced by 82% ± 25% (KLK8_1) or by 95% ± 5% (KLK8_2) (Fig. 5F and G), which indicated that proteolytic processing of L1 by KLK8 is a prerequisite for the exposure of the RG-1 epitope.

Since the subsequent action of both cyclophilin B and furin is required for RG-1 epitope exposure, the question remained whether KLK8 cleaves L1 before or after the structural changes caused by the chaperon cyclophilin B. To address this question, we examined whether cleavage of L1 in conditioned medium would occur in the presence of CsA, which would indicate KLK8 activity independently of cyclophilin B action. The assay was performed as described in the legend of Fig. 3 using concentrations of CsA that inhibited both infection and RG-1 exposure (Fig. 5F, G, and J). The generation of L1 A occurred to the same extents in the presence and absence of CsA (Fig. 5H and I). These findings indicate that L1 is cleaved by KLK8 independently of cyclophilin B.

DISCUSSION

The biochemical and cell-biological experiments presented here indicated the proteolytic processing of the major capsid protein L1 during HPV16 entry into host cells. In line with previous studies (23, 30, 32, 33), most of the proteolytic processing occurred in endolysosomes by cysteine cathepsins. Dispensable for infection, the cathepsin-mediated cleavages were likely the result of postuncoating L1 degradation and, in part, of an autophagic response to infection. In addition, three further cleavages were observed. The first of these was mediated by KLK8, a secreted serine protease. A prior conformational change through virus interaction with sulfated HS facilitated the extracellular, KLK8-mediated cleavage, which in turn allowed further conformational changes through viral interactions with cyclophilins and furin. Thus, our work demonstrated another crucial link in the complex chain of conformational changes in the virus particle that eventually leads to HPV16 internalization by endocytosis.

Previous studies followed the proteolysis of L1 primarily by the disappearance of full-length L1 in Western blotting (30–32). Extending this approach, our work focused on the appearance of distinct cleavage products. During the time course of infection, L1 was progressively processed, exhibiting at least eight distinct cleavage events. Most of these cleavages were suppressed by either elevating endosomal pH during infection or by inhibiting endosomal cysteine cathepsins, which suggested that most of the processing occurred in endolysosomes after internalization. The cathepsin-mediated cleavages neither facilitated nor suppressed infection and uncoating. Thus, cathepsin-mediated degradation was unlikely a part of the uncoating process. In addition, the autophagic response previously found to restrict infection (30, 60) was only in part responsible for the cathepsin-mediated degradation since inhibition of cathepsins did not facilitate infection and since cathepsin-mediated degradation was only reduced but not absent in cells blocked for autophagy. Taken together, it is likely that cathepsin-mediated degradation is a postuncoating event that presumably occurs in endolysosomal organelles.

At least three L1 cleavages were independent of cathepsins. Of those, one also did not require a low pH. This pH-independent cleavage occurred early during infection (2 to 4 h p.i.). Therefore, we hypothesized that it would already occur extracellularly. This notion was supported by the observation that the pH-independent cleavage was mediated by incubation of virus with secreted cellular material in the absence of cells. However, the cleavage appeared to be inefficient unless the virus was preincubated with heparin. Since the interaction of HPV16 PsV with highly sulfated HS facilitates infection by induction of a conformational change in virions (19, 70), it is likely that this conformational change exposed a protease consensus sequence of L1 that was at least partially obscured in the incoming HPV16 PsV.

Several lines of evidence indicated that the secreted serine protease KLK8 was responsible for the extracellular cleavage of HPV16 L1. Inhibitor studies demonstrated that it was mediated by a serine protease but did not involve cathepsins, matrix metalloproteases, or furin. In the two existing independent, large-scale RNAi screens, only KLK8 was commonly identified as a secreted serine protease required for HPV16 infection (4, 28). In this work, inhibition of HPV16 infection by RNAi-mediated silencing and

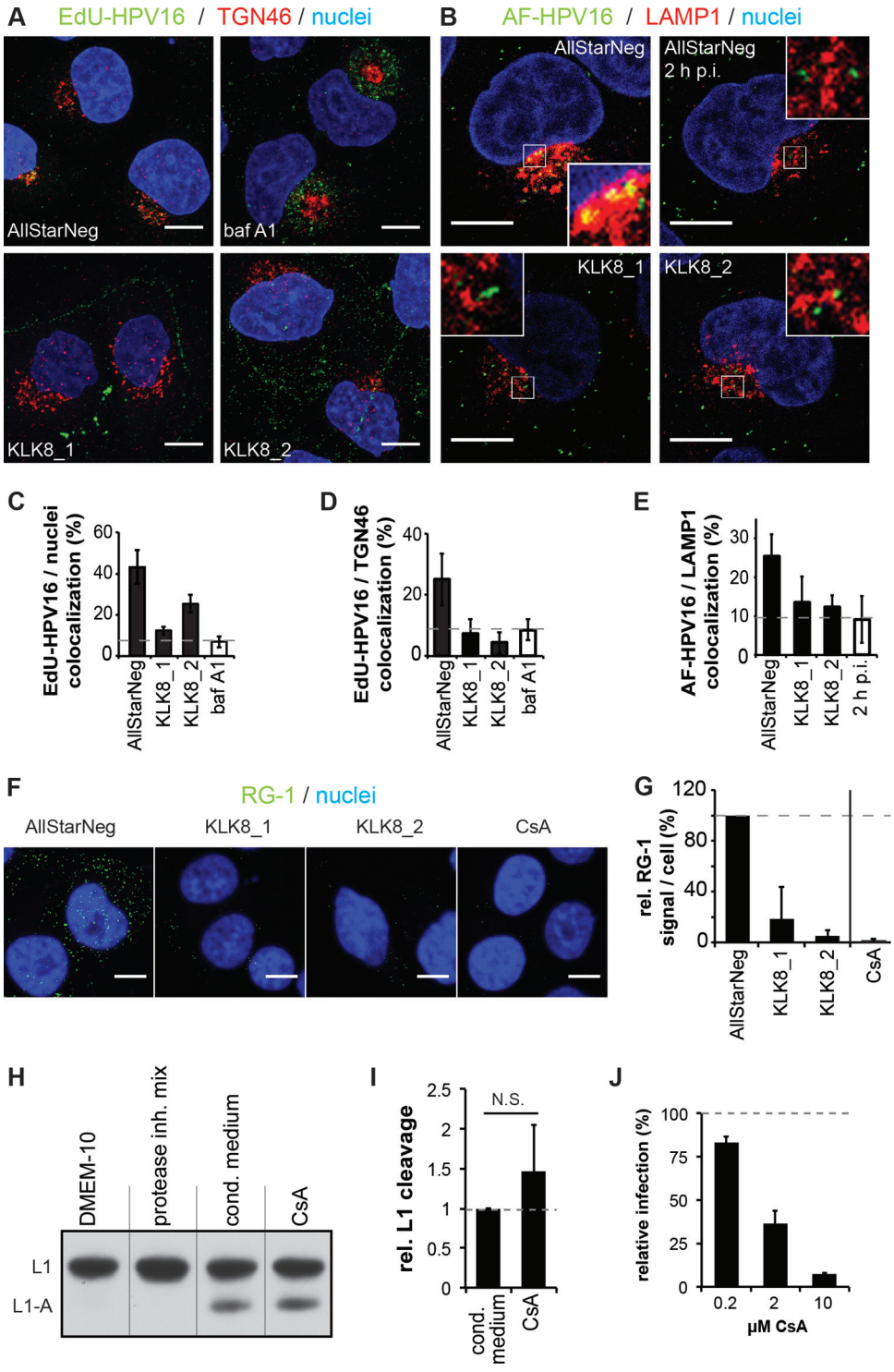

FIG 5 KLK8 is required for RG-1 epitope exposure. HeLa cells were reverse transfected with 10 nM concentrations of the indicated siRNAs directed against KLK8 or a nontargeting control (AllStarNeg). Cells were infected at 48 h posttransfection. Alternatively, cells were infected in the presence of bafilomycin A1 (Baf A1; 10 nM) or cyclosporine (CsA; 10 μM). (A) After infection with EdU-HPV16 for 20 h, cells were fixed, stained for EdU (viral DNA; green) and TGN46 (trans-Golgi network; red). The nucleus was visualized by Hoechst staining (blue). Depicted are maximum projections from confocal sections. (B) After infection with fluorescently labeled HPV16 PsV (AF-HPV16) for 8 h, cells were fixed and stained for LAMP1 (late endosomes and lysosomes; red). The nucleus was visualized by Hoechst staining (blue). Depicted are single confocal sections. (C) Quantification of EdU-HPV16 signals over nuclear staining from the experiment shown in panel A. Values are the percent signal overlap ± standard deviations of three independent experiments. (D) Quantification of EdU-HPV16 signals over TGN46 staining from the experiment described in panel A. Values are the percent signal overlap ± standard deviations of three independent experiments. (E) Quantification of AF-HPV16 signals over LAMP1 from the experiment shown in panel B. Values are the percent signal overlap ± standard deviations of three independent experiments. (F) After infection of cells with HPV16 PsV for 4 h, cells were immunostained with the RG-1 antibody for 2 h at 4°C (green) and subsequently fixed. The nucleus was visualized by Hoechst staining (blue). Depicted are maximum projections from confocal sections. (G) Quantification of

by the presence of antibodies confirmed the importance of KLK8. Decreased infection correlated with reduced cleavage in extracellular medium by immunodepletion of KLK8 or KLK8 inhibition with Zn^{2+} ions. Last but not least, the presence of conditioned medium restored infection in KLK8-depleted cells.

The KLK8-mediated cleavage appeared to be a prerequisite for an early step in the virus entry program. Based on the dispersed localization of HPV16 particles and vDNA, as well as on the decreased levels of colocalization with late endosomes, the Golgi compartment, or the nucleus in KLK8-depleted cells, a defect in internalization is likely. However, based on these results we cannot entirely rule out a very early defect in early intracellular trafficking. Perturbation of extracellular events in the HPV entry process does not necessarily prevent noninfectious internalization by bulk flow (21). That at least some, presumably noninfectious, internalization takes place in cells infected with large amounts of virus was indicated by the appearance of cathepsin-mediated cleavage products in cells treated with leupeptin. A different way to assess whether infectious internalization is inhibited by the absence of KLK8 is to determine whether the L1 cleavage would be important for the structural changes in the virion that facilitate transfer to an elusive secondary receptor and infectious uptake. These changes include the cyclophilin-mediated externalization of the L2 N terminus from the capsid interior (27) and the furin-mediated cleavage of this very N terminus (23). The completion of conformational changes in the virion is indicated by the exposure of the so-called RG-1 epitope (23, 24). Its absence in infected, KLK8-depleted cells supported the hypothesis that the conformational changes leading to receptor switching were facilitated by KLK8 prior to infectious internalization. That KLK8 worked independently of conformational changes induced by cyclophilins or furin was indicated by the efficient cleavage of L1 in the presence of cyclosporine or furin inhibitor. Therefore, it is likely that KLK8-mediated cleavage occurred prior to the action of cyclophilins and furin.

Based on these observations, we propose a model in which the induction of a first conformational change in HPV16 virions with heparan sulfates leads to the exposure of a KLK8 consensus cleavage site. Cleavage of L1 by KLK8 would then facilitate the externalization of the L2 N terminus by cyclophilins. This step would be followed by furin-mediated cleavage. All of these changes would then culminate in a virion that is primed for infectious internalization.

A prerequisite for this model is that KLK8 is present during HPV16 infection *in vivo*. The kallikrein family of secreted trypsin- or chymotrypsin-like serine proteases has roles in tissue homeostasis and cancerogenic pathologies (71). KLK8 itself is an understudied member of this family. Like other kallikreins, KLK8 exhibits a broad expression profile in many tissues. However, KLK8 is most prominently expressed in the brain, the mucosa, and the skin, where it has roles in tissue homeostasis, desquamation of cells, ECM remodelling, and wound healing (67, 72, 73). Since it has been speculated that HPV particles may be structurally primed for entry already at the site of assembly in the upper layers of the epithelium (25), authentic HPV might be cleaved by KLK8 at the site of desquamation prior to transmission. However, given the requirement for prior interaction with HS and the lack of direct evidence for structural priming of HPV, it may be more likely that KLK8 would act after virus attachment to the ECM/basement membrane or cells. KLK8's role in wound healing and ECM remodelling implies that it is actively present in considerable amounts during the initial HPV16 infection, which is thought to occur through microwounds in the epithelium (1).

Another prerequisite for our model is the presence of KLK8 cleavage sites in L1 that correlate with our experimental results. The molecular mass change of L1 indicated a KLK8 cleavage site that would generate a peptide of about 5 kDa from either the N or the C terminus. The consensus site for KLK8 has not been elucidated in full detail. However, based on sequence prediction and *in vitro* peptide proteolysis analysis, it is clear that KLK8 has a trypsin-like specificity (66, 68, 74, 75). The P1 position contains a positively charged amino acid, with Arg preferable over Lys (68, 74). In addition, a binding site of four amino acids in the substrate confers specificity with hydrophobic residues in P2 and P3 and preferably Ser/Thr or Phe/Tyr at P1′ (64). In the HPV16 L1 sequence, there are several such sites at the N and C termini that would generate peptides with calculated sizes of 4.6 to 9.7 kDa (Fig. 6A to C).

A cleavage at the C-terminal site 417R would generate pentamers that would be no longer covalently linked by the invading C-terminal arm's disulfide bond (between residues C175 and C428) (8, 76, 77) potentially generating a particle that is primed for uncoating by cyclophilins in the endosomal pathway. With a calculated size of 9.7 kDa, however, the cleaved peptide may be too large to account for our experimental results. The second C-terminal site (463R) would generate a peptide of about 4.6 kDa. Cleavage at 463R may also destabilize pentamer-pentamer contacts while leaving the covalent disulfide bond between pentamers intact.

Alternatively, the N terminus is thought to "plug" holes in the virion that are located in the canyon between pentamers (7). Cleavage at an N-terminal site may thus facilitate access of cyclophilins to the capsid lumen, which would allow the externalization of the L2 N terminus. The 64K site at the N terminus may be a particularly interesting candidate. Not only does cleavage at this site generate a peptide of 7 kDa, which would be in accord with the experimental results, it is also highly conserved among several PV types (Fig. 6A and C). Interestingly, the infectivity of HPV6 and

RG-1 immunofluorescence signal of samples from the experiment shown in panel F. Values (percents) are the amounts of RG-1 immunofluorescence signals per cell relative to the amounts for cells transfected with the nontargeting siRNAs (AllStarNeg) ± standard deviations of at least three independent experiments. (H) The experiment is as described in the legend of Fig. 3. ECM-bound, heparin-preincubated HPV16 PsV were incubated with conditioned medium in the presence or absence of CsA (10 μM). Samples were subjected to SDS-PAGE and Western blotting using the CAMVIR-1 antibody. (I) Quantification of the generation of L1 A with heparin-preincubated HPV16 from the experiment shown in panel H. Given are the relative amounts of L1 A signal intensities normalized to the value for the sample with conditioned medium without inhibitors. Data are the means of three independent experiments ± standard deviations. Statistical significance was tested by a two-tailed, independent *t* test. N.S., not significant. (J) HeLa cells were infected with HPV16-GFP in the presence or absence of CsA (cyclophilin inhibitor) at the indicated concentrations. The number of GFP-expressing (infected) cells was determined at 48 h p.i. by flow cytometry. Shown is the fraction of infected cells normalized relative to the number of solvent-treated cells. Values are the means of three independent experiments ± standard deviations. Scale bar, 10 μm.

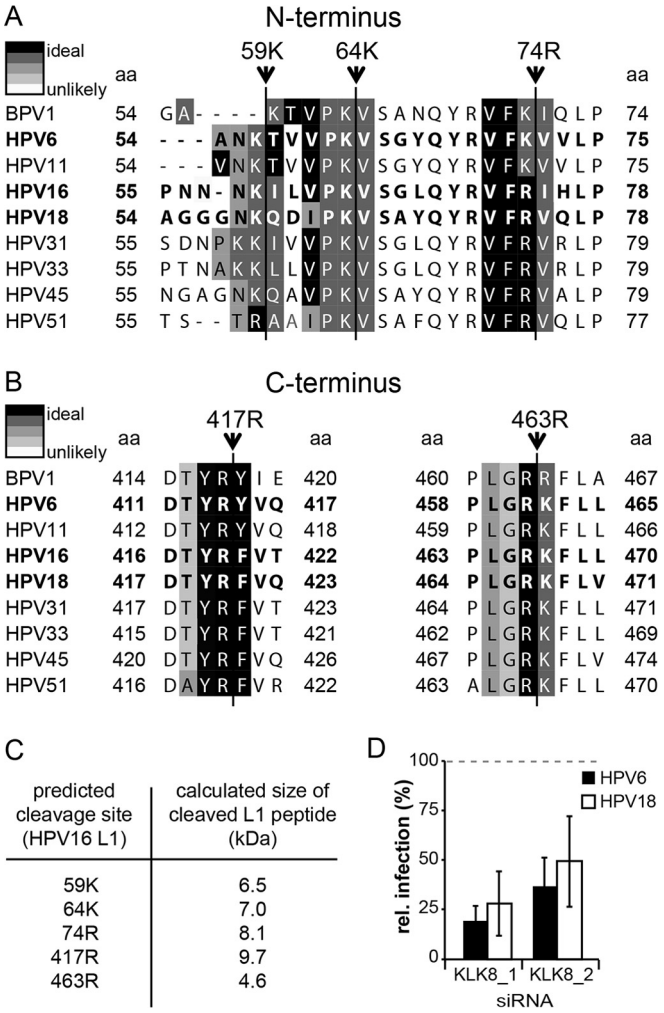

FIG 6 Predicted KLK8 cleavage sites in the L1 protein of various papillomavirus types. (A) Predicted cleavage sites in the L1 N-terminal-proximal sequence of the indicated papillomavirus types. Arrowheads indicate predicted cleavage sites. Amino acids at P1, P2, P3, and P1′ are depicted as ranging from highly favorable (ideal) to unfavorable (unlikely), according to the color legend. (B) Predicted cleavage sites in the L1 C-terminal-proximal sequence of the indicated papillomavirus types. The characterization of the amino acids is as described for panel A. (C) Calculated sizes (in kDa) of the potential HPV16 L1 peptides resulting from KLK8 cleavage at the consensus sites. (D) HeLa cells were reverse transfected with 10 nM siRNAs directed against KLK8 or the nontargeting control siRNA (AllStarNeg). Cells were infected with HPV6-GFP or HPV18-GFP at 48 h posttransfection. The number of GFP-expressing (infected) cells was determined at 48 h p.i. by flow cytometry. Depicted is the fraction of infected cells relative to the number of negative-control cells. Values are the means of three independent experiments ± standard deviations.

HPV18 was reduced in KLK8 knockdown cells, which is similar to the observations for HPV16 and provides the first evidence for a conserved role of KLK8 in HPV infection (Fig. 6D). To elucidate the actual cleavage site in HPV16 has proven to be challenging, most likely because both the N and C termini are required for stable assembly (78). For example, when we mutated one (74R) of the N-terminal KLK8 consensus sites in the L1 protein, a block of HPV16 assembly was observed (data not shown).

Therefore, future structural and functional studies are required to explore which site may be cleaved, whether KLK8 is unplugging holes in the virion by removing the L1 N terminus, and/or whether KLK8 facilitates uncoating in endosomes. In addition, the conservation of the potential KLK8 cleavage sites among several HPVs calls for future studies that address whether other HPV types require KLK8 or other KLK family members for entry into host cells.

ACKNOWLEDGMENTS

We thank J. Mercer for help with VV experiments and E. Weghake and A. Seeger for technical assistance in HPV PsV production. We thank members of the Schelhaas laboratory for their comments on the manuscript.

M.S. and C.C. were supported by the German Research Foundation (DFG, grants SCHE 1552/2-1 and EXC 1003 [partly]) and by the Portuguese Foundation for Science and Technology (Ph.D. grant SFRH/BD/45921/2008), respectively.

REFERENCES

1. **Doorbar J, Quint W, Banks L, Bravo IG, Stoler M, Broker TR, Stanley MA.** 2012. The biology and life-cycle of human papillomaviruses. Vaccine **30**(Suppl 5):F55–F70. http://dx.doi.org/10.1016/j.vaccine.2012.06.083.
2. **Parkin DM.** 2006. The global health burden of infection-associated cancers in the year 2002. Int J Cancer **118:**3030–3044. http://dx.doi.org/10.1002/ijc.21731.
3. **Brody H.** 2012. Human papillomavirus. Nature **488:**S1. http://dx.doi.org/10.1038/488S1a.
4. **Aydin I, Weber S, Snijder B, Samperio Ventayol P, Kuhbacher A, Becker M, Day PM, Schiller JT, Kann M, Pelkmans L, Helenius A, Schelhaas M.** 2014. Large scale RNAi reveals the requirement of nuclear envelope breakdown for nuclear import of human papillomaviruses. PLoS Pathog **10:**e1004162. http://dx.doi.org/10.1371/journal.ppat.1004162.
5. **Day PM, Schelhaas M.** 2014. Concepts of papillomavirus entry into host cells. Curr Opin Virol **4:**24–31. http://dx.doi.org/10.1016/j.coviro.2013.11.002.
6. **Holmgren SC, Patterson NA, Ozbun MA, Lambert PF.** 2005. The minor capsid protein L2 contributes to two steps in the human papillomavirus type 31 life cycle. J Virol **79:**3938–3948. http://dx.doi.org/10.1128/JVI.79.7.3938-3948.2005.
7. **Modis Y, Trus BL, Harrison SC.** 2002. Atomic model of the papillomavirus capsid. EMBO J **21:**4754–4762. http://dx.doi.org/10.1093/emboj/cdf494.
8. **Wolf M, Garcea RL, Grigorieff N, Harrison SC.** 2010. Subunit interactions in bovine papillomavirus. Proc Natl Acad Sci U S A **107:**6298–6303. http://dx.doi.org/10.1073/pnas.0914604107.
9. **Buck CB, Thompson CD, Pang YY, Lowy DR, Schiller JT.** 2005. Maturation of papillomavirus capsids. J Virol **79:**2839–2846. http://dx.doi.org/10.1128/JVI.79.5.2839-2846.2005.
10. **Cardone G, Moyer AL, Cheng N, Thompson CD, Dvoretzky I, Lowy DR, Schiller JT, Steven AC, Buck CB, Trus BL.** 2014. Maturation of the human papillomavirus 16 capsid. mBio **5**(4):e01104–14. http://dx.doi.org/10.1128/mBio.01104-14.
11. **Cerqueira C, Schelhaas M.** 2012. Principles of polyoma- and papillomavirus uncoating. Med Microbiol Immunol **201:**427–436. http://dx.doi.org/10.1007/s00430-012-0262-1.
12. **Buck CB, Pastrana DV, Lowy DR, Schiller JT.** 2005. Generation of HPV pseudovirions using transfection and their use in neutralization assays. Methods Mol Med **119:**445–462.
13. **Day PM, Thompson CD, Buck CB, Pang YY, Lowy DR, Schiller JT.** 2007. Neutralization of human papillomavirus with monoclonal antibodies reveals different mechanisms of inhibition. J Virol **81:**8784–8792. http://dx.doi.org/10.1128/JVI.00552-07.
14. **Johnson KM, Kines RC, Roberts JN, Lowy DR, Schiller JT, Day PM.** 2009. Role of heparan sulfate in attachment to and infection of the murine female genital tract by human papillomavirus. J Virol **83:**2067–2074. http://dx.doi.org/10.1128/JVI.02190-08.
15. **Broutian TR, Brendle SA, Christensen ND.** 2010. Differential binding patterns to host cells associated with particles of several human alphapapillomavirus types. J Gen Virol **91:**531–540. http://dx.doi.org/10.1099/vir.0.012732-0.
16. **Combita AL, Touze A, Bousarghin L, Sizaret PY, Munoz N, Coursaget P.** 2001. Gene transfer using human papillomavirus pseudovirions varies

according to virus genotype and requires cell surface heparan sulfate. FEMS Microbiol Lett **204:**183–188. http://dx.doi.org/10.1111/j.1574-6968.2001.tb10883.x.

17. **Giroglou T, Florin L, Schafer F, Streeck RE, Sapp M.** 2001. Human papillomavirus infection requires cell surface heparan sulfate. J Virol **75:**1565–1570. http://dx.doi.org/10.1128/JVI.75.3.1565-1570.2001.
18. **Kines RC, Thompson CD, Lowy DR, Schiller JT, Day PM.** 2009. The initial steps leading to papillomavirus infection occur on the basement membrane prior to cell surface binding. Proc Natl Acad Sci U S A **106:**20458–20463. http://dx.doi.org/10.1073/pnas.0908502106.
19. **Cerqueira C, Liu Y, Kuhling L, Chai W, Hafezi W, van Kuppevelt TH, Kuhn JE, Feizi T, Schelhaas M.** 2013. Heparin increases the infectivity of human papillomavirus type 16 independent of cell surface proteoglycans and induces L1 epitope exposure. Cell Microbiol **15:**1818–1836. http://dx.doi.org/10.1111/cmi.12150.
20. **Culp TD, Budgeon LR, Marinkovich MP, Meneguzzi G, Christensen ND.** 2006. Keratinocyte-secreted laminin 5 can function as a transient receptor for human papillomaviruses by binding virions and transferring them to adjacent cells. J Virol **80:**8940–8950. http://dx.doi.org/10.1128/JVI.00724-06.
21. **Selinka HC, Florin L, Patel HD, Freitag K, Schmidtke M, Makarov VA, Sapp M.** 2007. Inhibition of transfer to secondary receptors by heparan sulfate-binding drug or antibody induces noninfectious uptake of human papillomavirus. J Virol **81:**10970–10980. http://dx.doi.org/10.1128/JVI.00998-07.
22. **Bienkowska-Haba M, Patel HD, Sapp M.** 2009. Target cell cyclophilins facilitate human papillomavirus type 16 infection. PLoS Pathog **5:**e1000524. http://dx.doi.org/10.1371/journal.ppat.1000524.
23. **Richards RM, Lowy DR, Schiller JT, Day PM.** 2006. Cleavage of the papillomavirus minor capsid protein, L2, at a furin consensus site is necessary for infection. Proc Natl Acad Sci U S A **103:**1522–1527. http://dx.doi.org/10.1073/pnas.0508815103.
24. **Day PM, Gambhira R, Roden RB, Lowy DR, Schiller JT.** 2008. Mechanisms of human papillomavirus type 16 neutralization by l2 cross-neutralizing and l1 type-specific antibodies. J Virol **82:**4638–4646. http://dx.doi.org/10.1128/JVI.00143-08.
25. **Raff AB, Woodham AW, Raff LM, Skeate JG, Yan L, Da Silva DM, Schelhaas M, Kast WM.** 2013. The evolving field of human papillomavirus receptor research: a review of binding and entry. J Virol **87:**6062–6072. http://dx.doi.org/10.1128/JVI.00330-13.
26. **Schelhaas M, Shah B, Holzer M, Blattmann P, Kuhling L, Day PM, Schiller JT, Helenius A.** 2012. Entry of human papillomavirus type 16 by actin-dependent, clathrin- and lipid raft-independent endocytosis. PLoS Pathog **8:**e1002657. http://dx.doi.org/10.1371/journal.ppat.1002657.
27. **Bienkowska-Haba M, Williams C, Kim SM, Garcea RL, Sapp M.** 2012. Cyclophilins facilitate dissociation of the HPV16 capsid protein L1 from the L2/DNA complex following virus entry. J Virol **86:**9875–9887. http://dx.doi.org/10.1128/JVI.00980-12.
28. **Lipovsky A, Popa A, Pimienta G, Wyler M, Bhan A, Kuruvilla L, Guie MA, Poffenberger AC, Nelson CD, Atwood WJ, DiMaio D.** 2013. Genome-wide siRNA screen identifies the retromer as a cellular entry factor for human papillomavirus. Proc Natl Acad Sci U S A **110:**7452–7457. http://dx.doi.org/10.1073/pnas.1302164110.
29. **Day PM, Thompson CD, Schowalter RM, Lowy DR, Schiller JT.** 2013. Identification of a role for the trans-Golgi network in human papillomavirus 16 pseudovirus infection. J Virol **87:**3862–3870. http://dx.doi.org/10.1128/JVI.03222-12.
30. **Griffin LM, Cicchini L, Pyeon D.** 2013. Human papillomavirus infection is inhibited by host autophagy in primary human keratinocytes. Virology **437:**12–19. http://dx.doi.org/10.1016/j.virol.2012.12.004.
31. **Campos SK, Chapman JA, Deymier MJ, Bronnimann MP, Ozbun MA.** 2012. Opposing effects of bacitracin on human papillomavirus type 16 infection: enhancement of binding and entry and inhibition of endosomal penetration. J Virol **86:**4169–4181. http://dx.doi.org/10.1128/JVI.05493-11.
32. **Calton CM, Schlegel AM, Chapman JA, Campos SK.** 2013. Human papillomavirus type 16 does not require cathepsin L or B for infection. J Gen Virol **94:**1865–1869. http://dx.doi.org/10.1099/vir.0.053694-0.
33. **Dabydeen SA, Meneses PI.** 2009. The role of NH4Cl and cysteine proteases in human papillomavirus type 16 infection. Virol J **6:**109. http://dx.doi.org/10.1186/1743-422X-6-109.
34. **Snijder B, Sacher R, Ramo P, Liberali P, Mench K, Wolfrum N, Burleigh L, Scott CC, Verheije MH, Mercer J, Moese S, Heger T, Theusner K, Jurgeit A, Lamparter D, Balistreri G, Schelhaas M, De Haan CA, Marjomaki V, Hyypia T, Rottier PJ, Sodeik B, Marsh M, Gruenberg J, Amara A, Greber U, Helenius A, Pelkmans L.** 2012. Single-cell analysis of population context advances RNAi screening at multiple levels. Mol Syst Biol **8:**579. http://dx.doi.org/10.1038/msb.2012.9.
35. **Boukamp P, Petrussevska RT, Breitkreutz D, Hornung J, Markham A, Fusenig NE.** 1988. Normal keratinization in a spontaneously immortalized aneuploid human keratinocyte cell line. J Cell Biol **106:**761–771. http://dx.doi.org/10.1083/jcb.106.3.761.
36. **Sapp M, Kraus U, Volpers C, Snijders PJ, Walboomers JM, Streeck RE.** 1994. Analysis of type-restricted and cross-reactive epitopes on virus-like particles of human papillomavirus type 33 and in infected tissues using monoclonal antibodies to the major capsid protein. J Gen Virol **75:**3375–3383. http://dx.doi.org/10.1099/0022-1317-75-12-3375.
37. **Gambhira R, Karanam B, Jagu S, Roberts JN, Buck CB, Bossis I, Alphs H, Culp T, Christensen ND, Roden RB.** 2007. A protective and broadly cross-neutralizing epitope of human papillomavirus L2. J Virol **81:**13927–13931. http://dx.doi.org/10.1128/JVI.00936-07.
38. **Buck CB, Thompson CD.** 2007. Production of papillomavirus-based gene transfer vectors. Curr Protoc Cell Biol Chapter 26:Unit 26.1. http://dx.doi.org/10.1002/0471143030.cb2601s37.
39. **Pastrana DV, Buck CB, Pang YY, Thompson CD, Castle PE, FitzGerald PC, Kruger Kjaer S, Lowy DR, Schiller JT.** 2004. Reactivity of human sera in a sensitive, high-throughput pseudovirus-based papillomavirus neutralization assay for HPV16 and HPV18. Virology **321:**205–216. http://dx.doi.org/10.1016/j.virol.2003.12.027.
40. **Roberts JN, Buck CB, Thompson CD, Kines R, Bernardo M, Choyke PL, Lowy DR, Schiller JT.** 2007. Genital transmission of HPV in a mouse model is potentiated by nonoxynol-9 and inhibited by carrageenan. Nat Med **13:**857–861. http://dx.doi.org/10.1038/nm1598.
41. **Day PM, Baker CC, Lowy DR, Schiller JT.** 2004. Establishment of papillomavirus infection is enhanced by promyelocytic leukemia protein (PML) expression. Proc Natl Acad Sci U S A **101:**14252–14257. http://dx.doi.org/10.1073/pnas.0404229101.
42. **Schelhaas M, Ewers H, Rajamaki ML, Day PM, Schiller JT, Helenius A.** 2008. Human papillomavirus type 16 entry: retrograde cell surface transport along actin-rich protrusions. PLoS Pathog **4:**e1000148. http://dx.doi.org/10.1371/journal.ppat.1000148.
43. **Mercer J, Helenius A.** 2008. Vaccinia virus uses macropinocytosis and apoptotic mimicry to enter host cells. Science **320:**531–535. http://dx.doi.org/10.1126/science.1155164.
44. **McLean CS, Churcher MJ, Meinke J, Smith GL, Higgins G, Stanley M, Minson AC.** 1990. Production and characterisation of a monoclonal antibody to human papillomavirus type 16 using recombinant vaccinia virus. J Clin Pathol **43:**488–492. http://dx.doi.org/10.1136/jcp.43.6.488.
45. **Day PM, Lowy DR, Schiller JT.** 2003. Papillomaviruses infect cells via a clathrin-dependent pathway. Virology **307:**1–11. http://dx.doi.org/10.1016/S0042-6822(02)00143-5.
46. **Selinka HC, Giroglou T, Sapp M.** 2002. Analysis of the infectious entry pathway of human papillomavirus type 33 pseudovirions. Virology **299:**279–287. http://dx.doi.org/10.1006/viro.2001.1493.
47. **Smith JL, Campos SK, Wandinger-Ness A, Ozbun MA.** 2008. Caveolin-1-dependent infectious entry of human papillomavirus type 31 in human keratinocytes proceeds to the endosomal pathway for pH-dependent uncoating. J Virol **82:**9505–9512. http://dx.doi.org/10.1128/JVI.01014-08.
48. **Spoden G, Freitag K, Husmann M, Boller K, Sapp M, Lambert C, Florin L.** 2008. Clathrin- and caveolin-independent entry of human papillomavirus type 16–involvement of tetraspanin-enriched microdomains (TEMs). PLoS One **3:**e3313. http://dx.doi.org/10.1371/journal.pone.0003313.
49. **Blum JS, Diaz R, Diment S, Fiani M, Mayorga L, Rodman JS, Stahl PD.** 1989. Proteolytic processing in endosomal vesicles. Cold Spring Harbor Symp Quant Biol **54:**287–292. http://dx.doi.org/10.1101/SQB.1989.054.01.036.
50. **Guha S, Padh H.** 2008. Cathepsins: fundamental effectors of endolysosomal proteolysis. Indian J Biochem Biophys **45:**75–90.
51. **Turk V, Stoka V, Vasiljeva O, Renko M, Sun T, Turk B, Turk D.** 2012. Cysteine cathepsins: from structure, function and regulation to new frontiers. Biochim Biophys Acta **1824:**68–88. http://dx.doi.org/10.1016/j.bbapap.2011.10.002.
52. **Barrett AJ, Kembhavi AA, Brown MA, Kirschke H, Knight CG, Tamai M, Hanada K.** 1982. L-*trans*-Epoxysuccinyl-leucylamido(4-guanidino)butane (E-64) and its analogues as inhibitors of cysteine proteinases including cathepsins B, H and L. Biochem J **201:**189–198.

53. **Aoyagi T, Takeuchi T, Matsuzaki A, Kawamura K, Kondo S.** 1969. Leupeptins, new protease inhibitors from *Actinomycetes*. J Antibiotics **22:** 283–286. http://dx.doi.org/10.7164/antibiotics.22.283.
54. **Otto HH, Schirmeister T.** 1997. Cysteine proteases and their inhibitors. Chem Rev **97:**133–172. http://dx.doi.org/10.1021/cr950025u.
55. **Kirschke H, Shaw E.** 1981. Rapid interaction of cathepsin L by Z-Phe-PheCHN12 and Z-Phe-AlaCHN2. Biochem Biophys Res Commun **101:** 454–458. http://dx.doi.org/10.1016/0006-291X(81)91281-X.
56. **Kirschke H, Wikstrom P, Shaw E.** 1988. Active center differences between cathepsins L and B: the S1 binding region. FEBS Lett **228:**128–130. http://dx.doi.org/10.1016/0014-5793(88)80600-8.
57. **Murata M, Miyashita S, Yokoo C, Tamai M, Hanada K, Hatayama K, Towatari T, Nikawa T, Katunuma N.** 1991. Novel epoxysuccinyl peptides. Selective inhibitors of cathepsin B, in vitro. FEBS Lett **280:**307–310.
58. **Buttle DJ, Murata M, Knight CG, Barrett AJ.** 1992. CA074 methyl ester: a proinhibitor for intracellular cathepsin B. Arch Biochem Biophys **299:** 377–380. http://dx.doi.org/10.1016/0003-9861(92)90290-D.
59. **Levine B, Kroemer G.** 2008. Autophagy in the pathogenesis of disease. Cell **132:**27–42. http://dx.doi.org/10.1016/j.cell.2007.12.018.
60. **Surviladze Z, Sterk RT, DeHaro SA, Ozbun MA.** 2013. Cellular entry of human papillomavirus type 16 involves activation of the phosphatidylinositol 3-kinase/Akt/mTOR pathway and inhibition of autophagy. J Virol **87:**2508–2517. http://dx.doi.org/10.1128/JVI.02319-12.
61. **Bronnimann MP, Chapman JA, Park CK, Campos SK.** 2013. A transmembrane domain and GxxxG motifs within L2 are essential for papillomavirus infection. J Virol **87:**464–473. http://dx.doi.org/10.1128/JVI.01539-12.
62. **Kazmirowski HG.** 1971. Synthesis of antiproteolytic effective derivatives of benzosulfofluoride. Die Pharmazie **26:**390–393. (In German.)
63. **Surviladze Z, Dziduszko A, Ozbun MA.** 2012. Essential roles for soluble virion-associated heparan sulfonated proteoglycans and growth factors in human papillomavirus infections. PLoS Pathog **8:**e1002519. http://dx.doi.org/10.1371/journal.ppat.1002519.
64. **Eissa A, Amodeo V, Smith CR, Diamandis EP.** 2011. Kallikrein-related peptidase-8 (KLK8) is an active serine protease in human epidermis and sweat and is involved in a skin barrier proteolytic cascade. J Biol Chem **286:**687–706. http://dx.doi.org/10.1074/jbc.M110.125310.
65. **Inoue N, Kuwae K, Ishida-Yamamoto A, Iizuka H, Shibata M, Yoshida S, Kato K, Shiosaka S.** 1998. Expression of neuropsin in the keratinizing epithelial tissue-immunohistochemical analysis of wild-type and nude mice. J Invest Dermatol **110:**923–931. http://dx.doi.org/10.1046/j.1523-1747.1998.00212.x.
66. **Shimizu C, Yoshida S, Shibata M, Kato K, Momota Y, Matsumoto K, Shiosaka T, Midorikawa R, Kamachi T, Kawabe A, Shiosaka S.** 1998. Characterization of recombinant and brain neuropsin, a plasticity-related serine protease. J Biol Chem **273:**11189–11196. http://dx.doi.org/10.1074/jbc.273.18.11189.
67. **Rajapakse S, Ogiwara K, Takano N, Moriyama A, Takahashi T.** 2005. Biochemical characterization of human kallikrein 8 and its possible involvement in the degradation of extracellular matrix proteins. FEBS Lett **579:**6879–6884. http://dx.doi.org/10.1016/j.febslet.2005.11.039.
68. **Kishi T, Cloutier SM, Kundig C, Deperthes D, Diamandis EP.** 2006. Activation and enzymatic characterization of recombinant human kallikrein 8. Biol Chem **387:**723–731. http://dx.doi.org/10.1515/BC.2006.091.
69. **Ishii Y, Tanaka K, Kondo K, Takeuchi T, Mori S, Kanda T.** 2010. Inhibition of nuclear entry of HPV16 pseudovirus-packaged DNA by an anti-HPV16 L2 neutralizing antibody. Virology **406:**181–188. http://dx.doi.org/10.1016/j.virol.2010.07.019.
70. **Richards KF, Mukherjee S, Bienkowska-Haba M, Pang J, Sapp M.** 2014. Human papillomavirus species-specific interaction with the basement membrane-resident non-heparan sulfate receptor. Viruses **6:**4856–4879. http://dx.doi.org/10.3390/v6124856.
71. **Borgono CA, Michael IP, Diamandis EP.** 2004. Human tissue kallikreins: physiologic roles and applications in cancer. Mol Cancer Res **2:**257–280.
72. **Kitayoshi H, Inoue N, Kuwae K, Chen ZL, Sato H, Ohta T, Hosokawa K, Itami S, Yoshikawa K, Yoshida S, Shiosaka S.** 1999. Effect of 12-O-tetradecanoyl-phorbol ester and incisional wounding on neuropsin mRNA and its protein expression in murine skin. Arch Dermatol Res **291:**333–338. http://dx.doi.org/10.1007/s004030050418.
73. **Kishibe M, Bando Y, Tanaka T, Ishida-Yamamoto A, Iizuka H, Yoshida S.** 2012. Kallikrein-related peptidase 8-dependent skin wound healing is associated with upregulation of kallikrein-related peptidase 6 and PAR2. J Invest Dermatol **132:**1717–1724. http://dx.doi.org/10.1038/jid.2012.18.
74. **Yoon H, Laxmikanthan G, Lee J, Blaber SI, Rodriguez A, Kogot JM, Scarisbrick IA, Blaber M.** 2007. Activation profiles and regulatory cascades of the human kallikrein-related peptidases. J Biol Chem **282:**31852–31864. http://dx.doi.org/10.1074/jbc.M705190200.
75. **Scott FL, Sun J, Whisstock JC, Kato K, Bird PI.** 2007. SerpinB6 is an inhibitor of kallikrein-8 in keratinocytes. J Biochem **142:**435–442. http://dx.doi.org/10.1093/jb/mvm156.
76. **Ishii Y, Tanaka K, Kanda T.** 2003. Mutational analysis of human papillomavirus type 16 major capsid protein L1: the cysteines affecting the intermolecular bonding and structure of L1-capsids. Virology **308:**128–136. http://dx.doi.org/10.1016/S0042-6822(02)00099-5.
77. **Sapp M, Fligge C, Petzak I, Harris JR, Streeck RE.** 1998. Papillomavirus assembly requires trimerization of the major capsid protein by disulfides between two highly conserved cysteines. J Virol **72:**6186–6189.
78. **Chen XS, Garcea RL, Goldberg I, Casini G, Harrison SC.** 2000. Structure of small virus-like particles assembled from the L1 protein of human papillomavirus 16. Mol Cell **5:**557–567. http://dx.doi.org/10.1016/S1097-2765(00)80449-9.